シンクロトロン放射光を用いた単分散ミセルの構造解析
–プラト ニックミセルの提案–

Characterizing Self-Assembled Nanoparticles Employed in DDS

Kazuo Sakuraui
Dep. of Chemistry & Biochemistry
University of Kitakyushu

奈良先端大院　12月2日

Outline

Self-assembly and Drug Delivery System (DDS)

Strength of SAS technique in exploring DDS particles

Examples from Our Recent Studies

- Polymeric Micelle for Delivering Hydrophobic Drugs

J. Am. Chem. Soc., 135 (7), 2574–2582(2013)
Macromolecules, (Web): July 23, (2012)
J. Phys. Chem. B, 8241–8250, (2012)
Polymer Journal, 44, 240-244 (2012)

- Monodisperse Calixarene Micelles for DNA Delivery

Langmuir, *28* (6), 3092–3101, (2012)
Bull. Chem. Soc. Jpn. 354-359 (2012)
Langmuir, 29 (45), 13666–13675,（2013）
Chem. Commun.,49, 3052-3054,（2013）

- Short DNA DDS for Immune-stimulation and Gene Silencing

J. Phys. Chem. B,, *116* (1), 87–94 (2012)
Molecular Therapy (Nature), 20, 1234-1241 (2012)
Journal of Controlled Release, 155-161 (2011)
Bioconjugate Chemistry 22 9-15, (2011)
J. Am. Chem. Soc. 126, 8372-8373, (2004)

Outline

Self-assembly and Drug Delivery System (DDS)

Strength of SAS technique in exploring DDS particles

Examples from Our Recent Studies

- Polymeric Micelle for Delivering Hydrophobic Drugs

J. Am. Chem. Soc., 135 (7), 2574–2582(2013)
Macromolecules, (Web): July 23, (2012)
J. Phys. Chem. B, 8241–8250, (2012)
Polymer Journal, 44, 240-244 (2012)

- Monodisperse Calixarene Micelles for DNA Delivery

Langmuir, *28* (6), 3092–3101, (2012)
Bull. Chem. Soc. Jpn. 354-359 (2012)
Langmuir, 29 (45), 13666–13675,（2013）
Chem. Commun.,49, 3052-3054,（2013）

- Short DNA DDS for Immune-stimulation and Gene Silencing

J. Phys. Chem. B,, *116* (1), 87–94 (2012)
Molecular Therapy (Nature), 20, 1234-1241 (2012)
Journal of Controlled Release, 155-161 (2011)
Bioconjugate Chemistry 22 9-15, (2011)
J. Am. Chem. Soc. 126, 8372-8373, (2004)

DDS Needs Very Sophisticated Chemistry: Self-assembly and Supermolecues

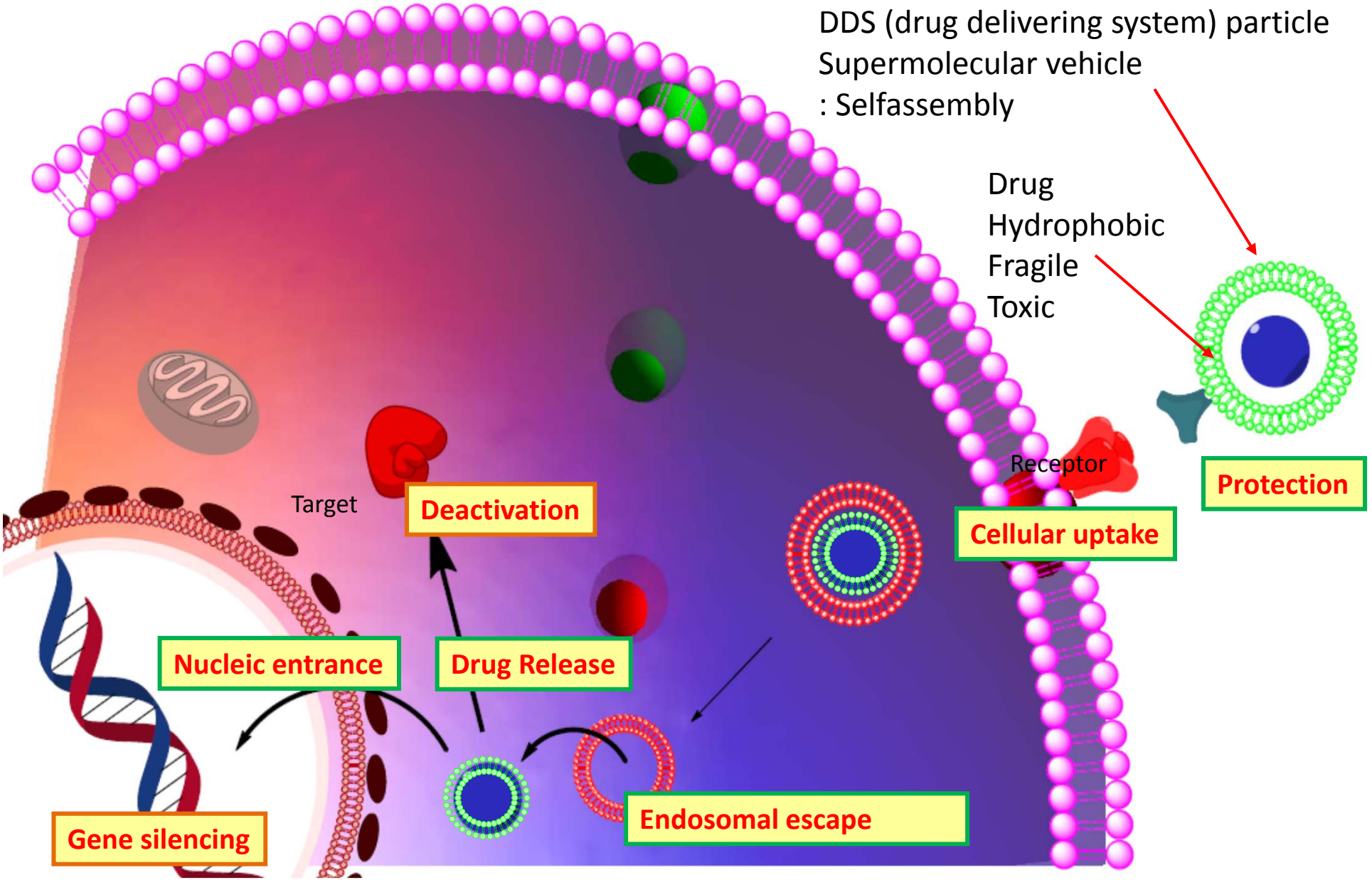

Example: Therapeutic Efficacy Strongly Depends on its Size

Ingestion: Enhanced Permeability and Retention

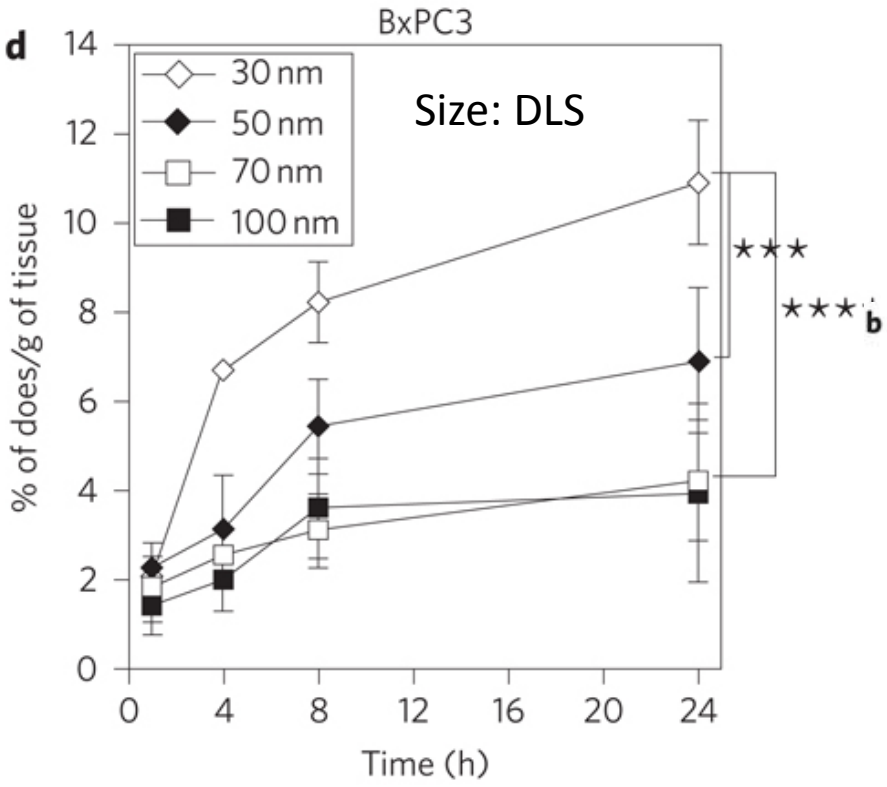

Tumour accumulation with different diameters.

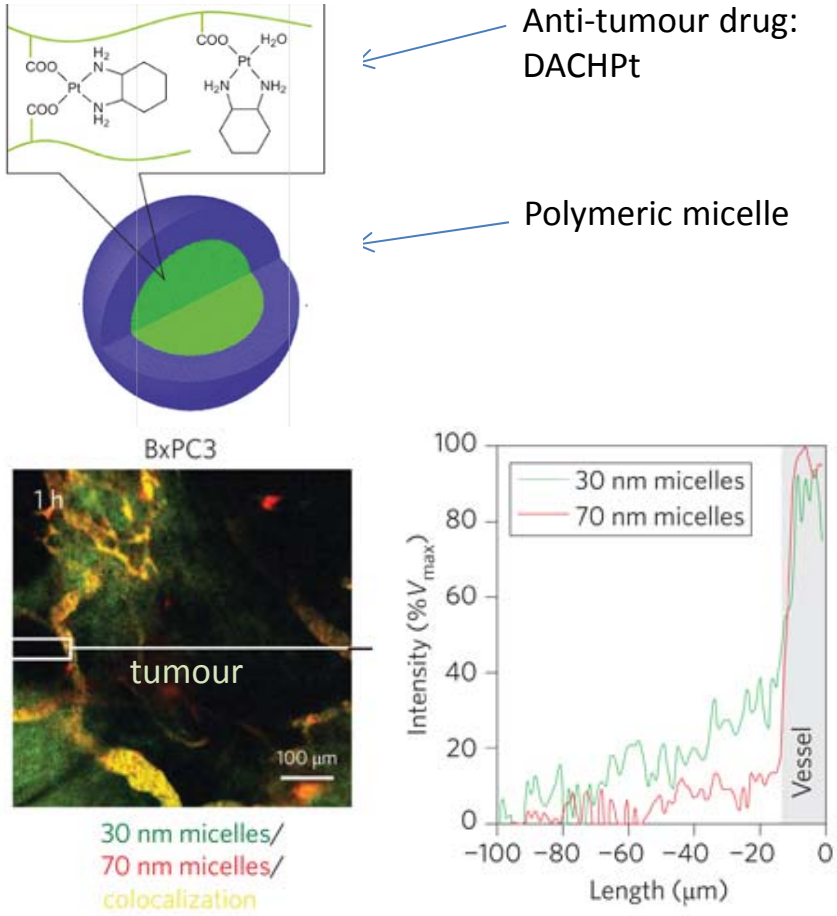

In vivo real-time microdistribution of DACHPt/m with different diameters in tumours

The sizes less than 100 nm are very good for SAS.

Accumulation of sub-100 nm polymeric micelles in poorly permeable tumours depends on size
K. Kataoka et al., *Nature Nanotechnology* (2011)

大きさの異なる２種類の金粒子

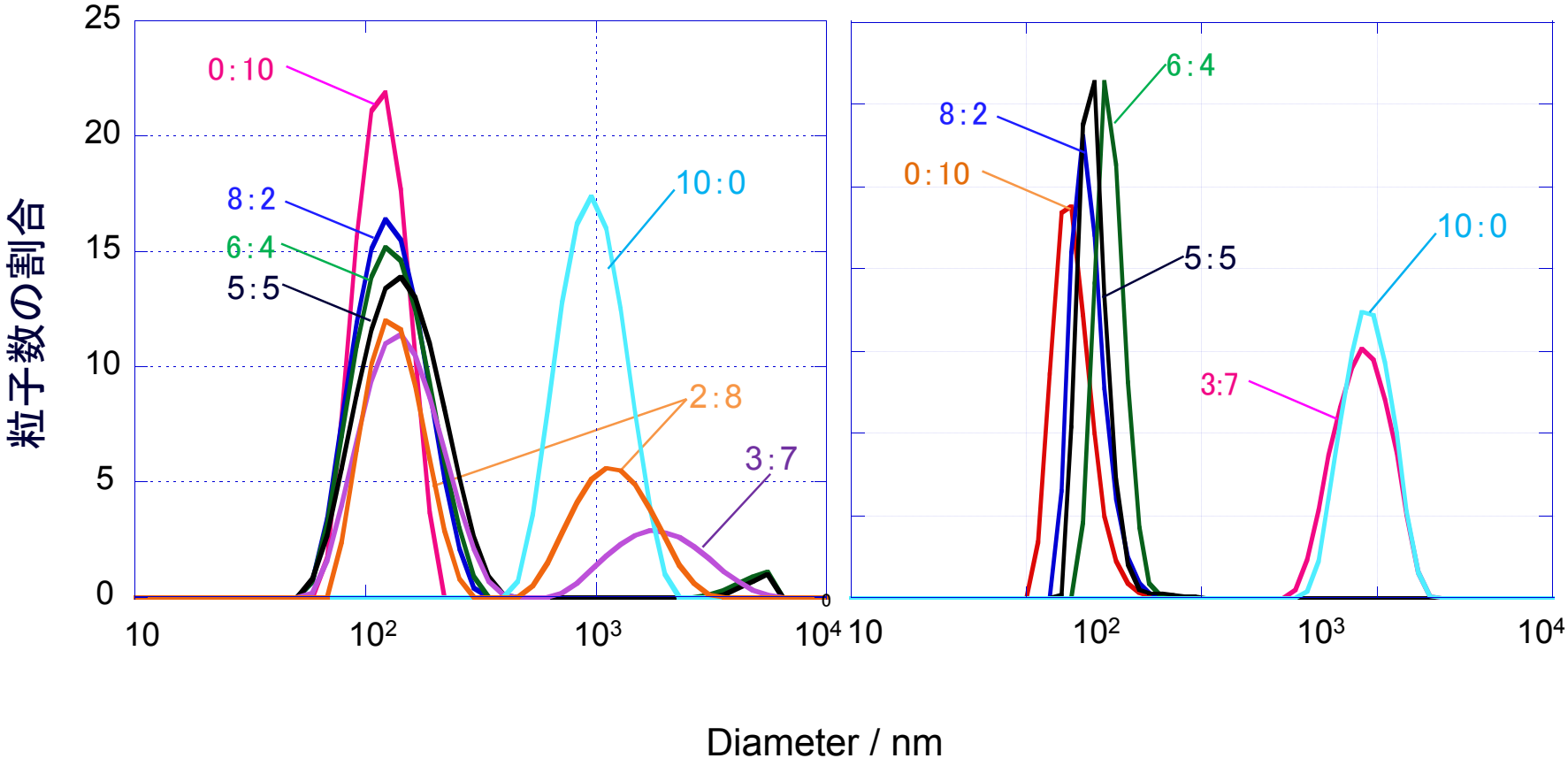

Goal:
Precise Structural Analysis and Visualization of DDS nano-particles by use of
SAXS with combination of FFF/MALS

Molecular Design
Product Control
FDA approval
Fundamental Physics and Chemistry

People are really care about what is going to be injected into your blood vessel.

What I am afraid is what's inside !!.

FFF: filed flow fluctuation,
MALS: multi-angle light scattering

aFFF coupled with MALS

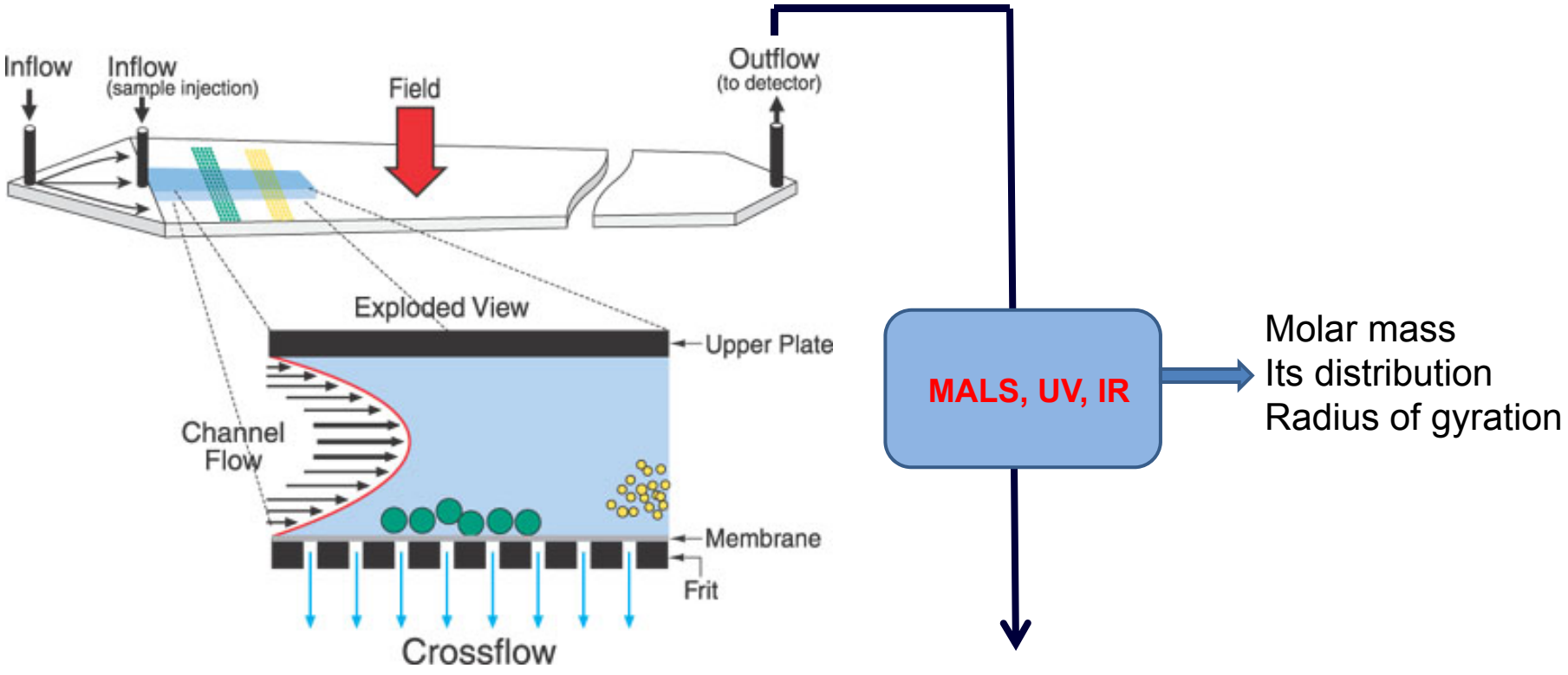

Asymmetric-Flow Field-Flow-Fractionation (aFFF or FFF) is a one-phase chromatography.

Channel flow + cross flow. i.e., No matrix material (do not care adsorption)

Optical purification of SLS in aqueous solutions.

aFFF (Asymmetric flow field flow fractionation)

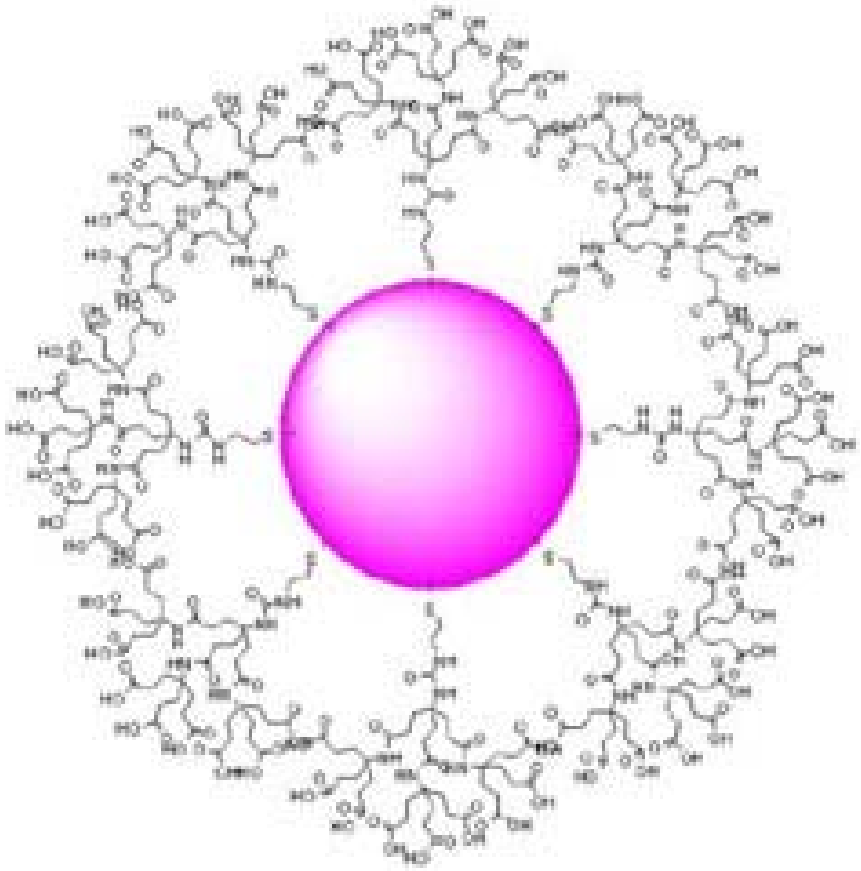

Dendron-Stabilized Gold Nanoparticles

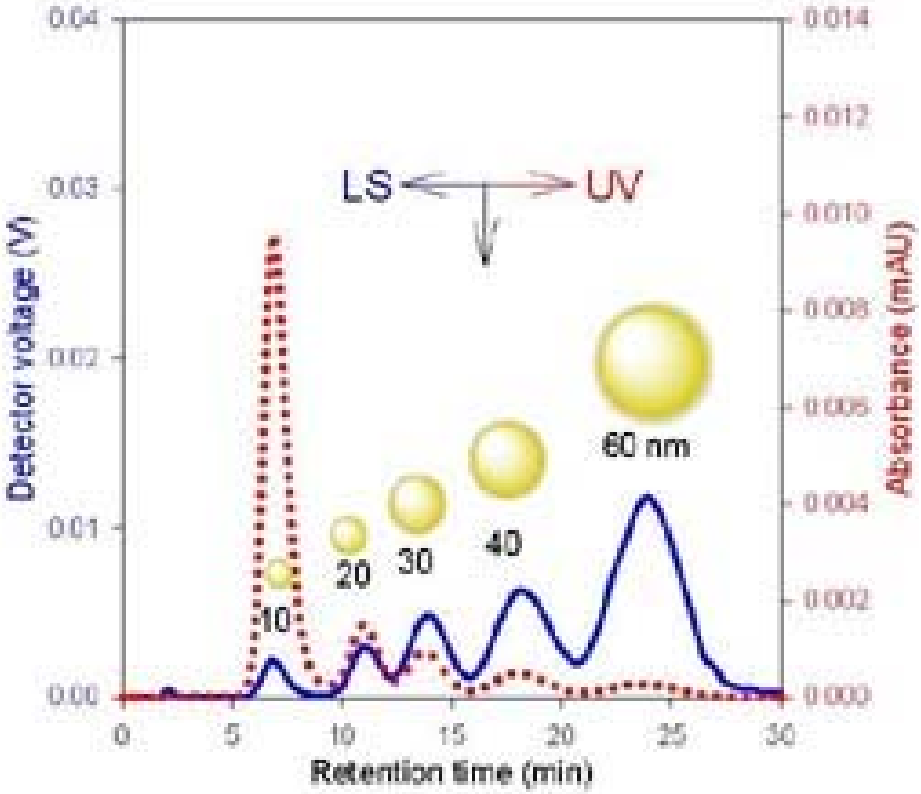

AFFF fractograms of M5 (10, 20, 30, 40, and 60 nm) AuNP mixture in 0.02 % NaN_3 mobile phase. 90° MALS (LS) / UV traces (—)/(•••)

De-Hao TSai (in Hackley's group) *JACS* 2011, 8884

DLSとaFFF/MALSの比較j

Figure 6. Examples of size distribution for PS-latex nanoparticle suspensions determined by DLS using cumulant analytical method. (**a**) STADEX SC-0110-D and (**b**) T0625.

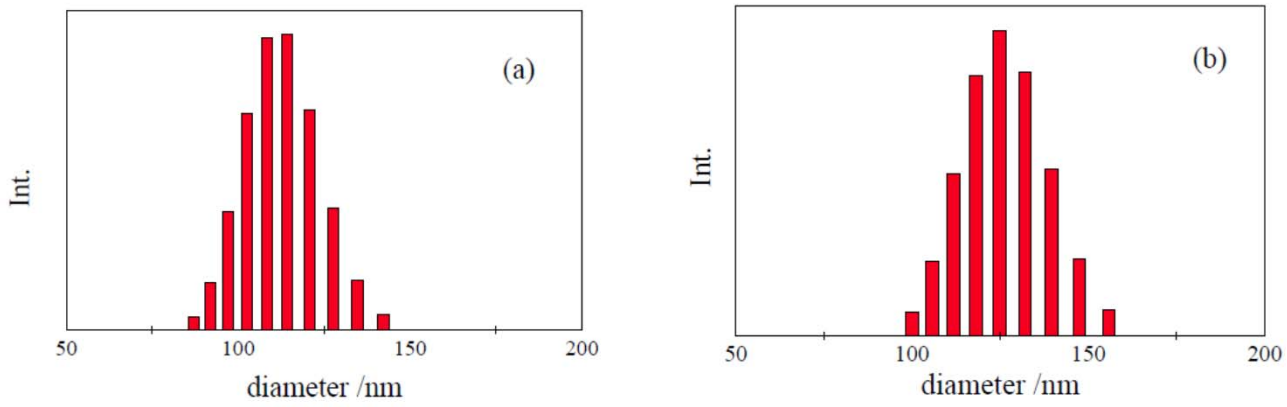

Figure 7. Examples of size distribution for PS-latex nanoparticle dispersions determined by AFFFF-MALS. (**a**) STADEX SC-0110-D and (**b**) T0625.

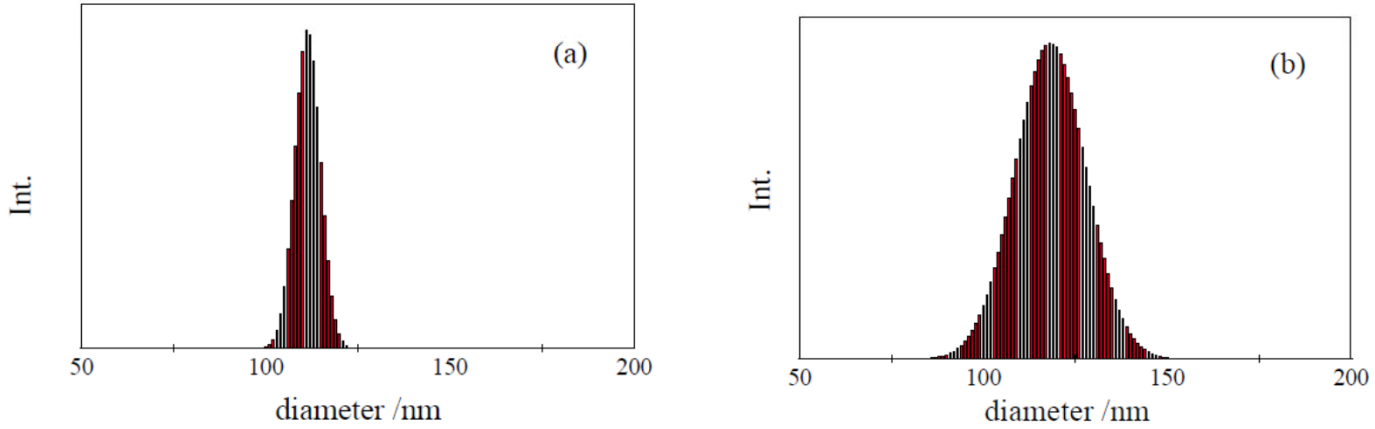

Nanomaterials 2012, 2, 15-30

SAXS at SPring-8 and our set-up

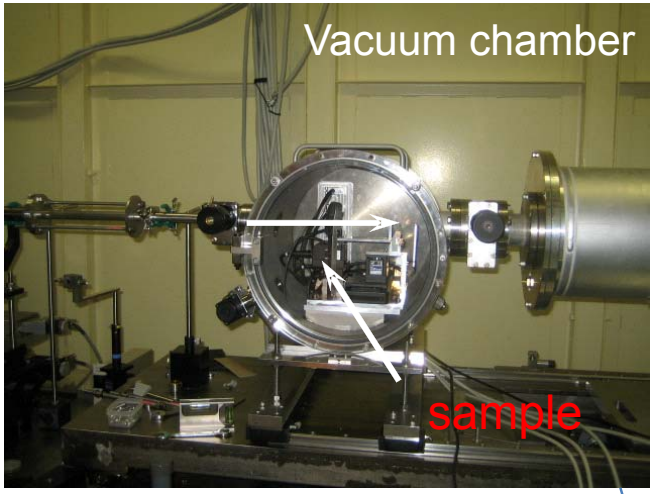

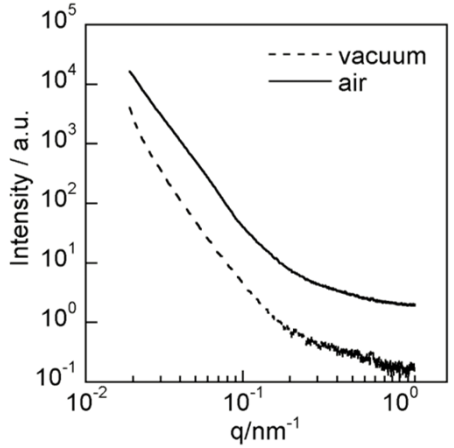

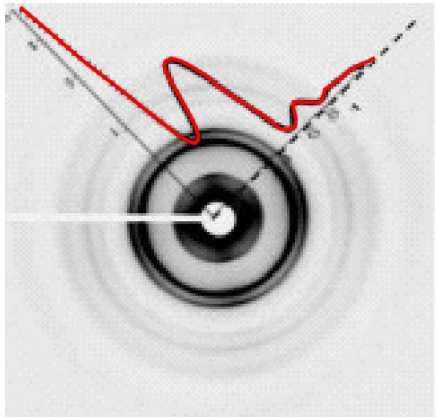

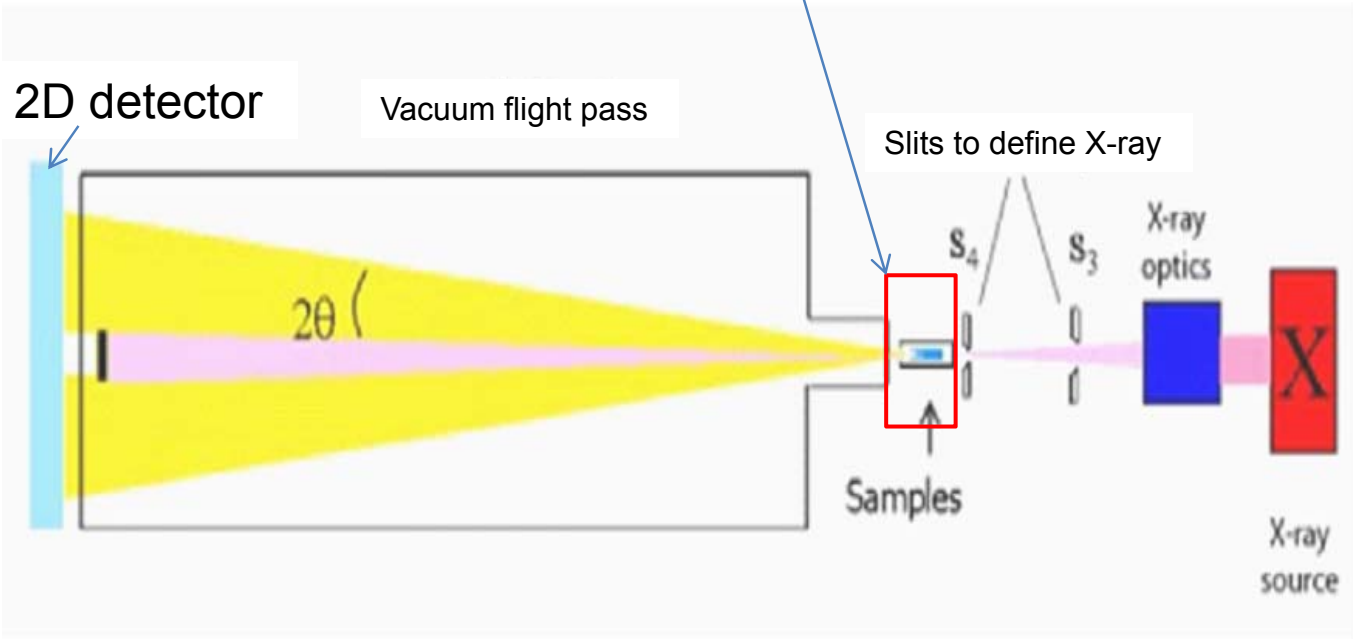

Scattering angle < 2 degree => 1 – 100 nm
Small angle X-ray scattering (SAXS)

$$q = \frac{2\pi}{\lambda}\sin\theta \qquad d \propto \frac{1}{q}$$

WAXS vs. SAXS

Scattering angle 5 – 25 degree => less than 0.5 nm
Wide angle X-ray scattering (WAXS, XRD)

Structural Factor (構造因子): distances between atoms.

Scattering angle < 2 degree => 1 – 100 nm
Small angle X-ray scattering (SAXS)

Structural Factor (構造因子): distance between particles

Form Factor (形状因子): shape

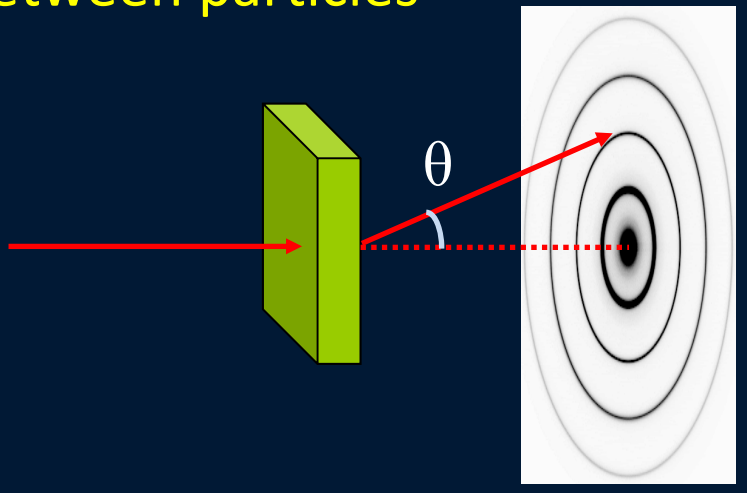

Spherical waves from many points => Structural factor

Intuitive understanding of diffraction

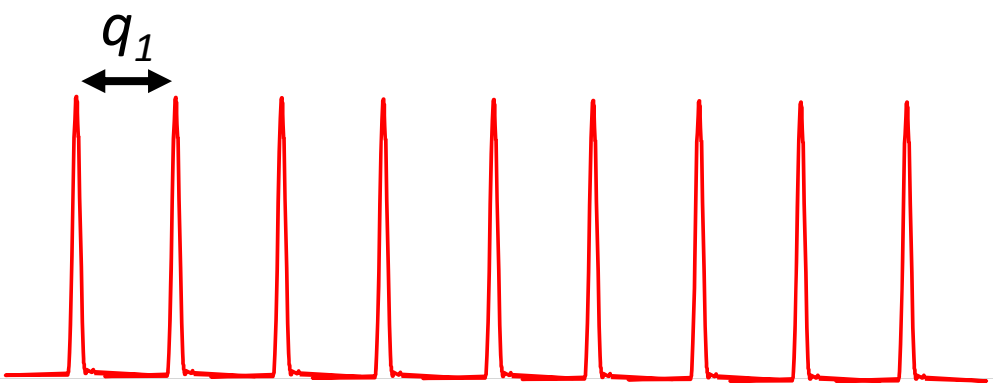

$$d \propto \frac{1}{q}$$

Brigg's low

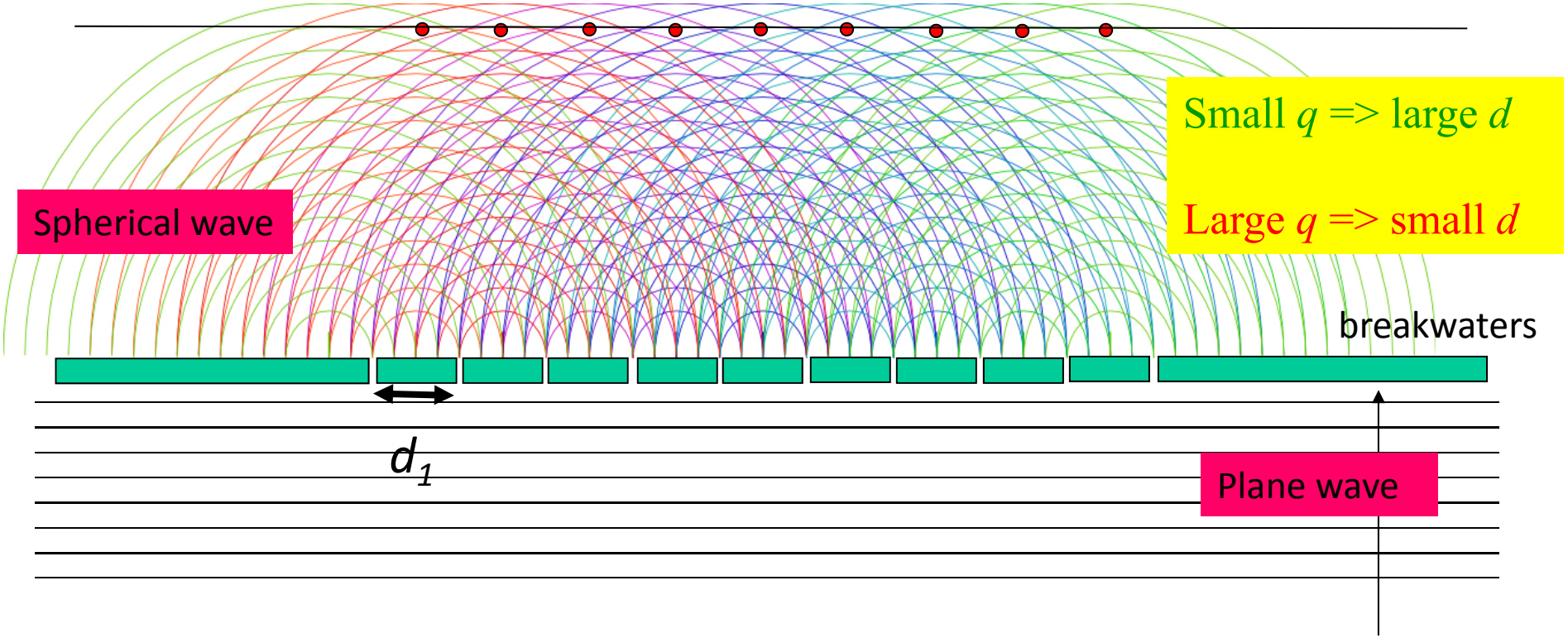

Diffraction from a slit with finite width => form factor

q: magnitude of the scattering vector
=> distance from the scattering center

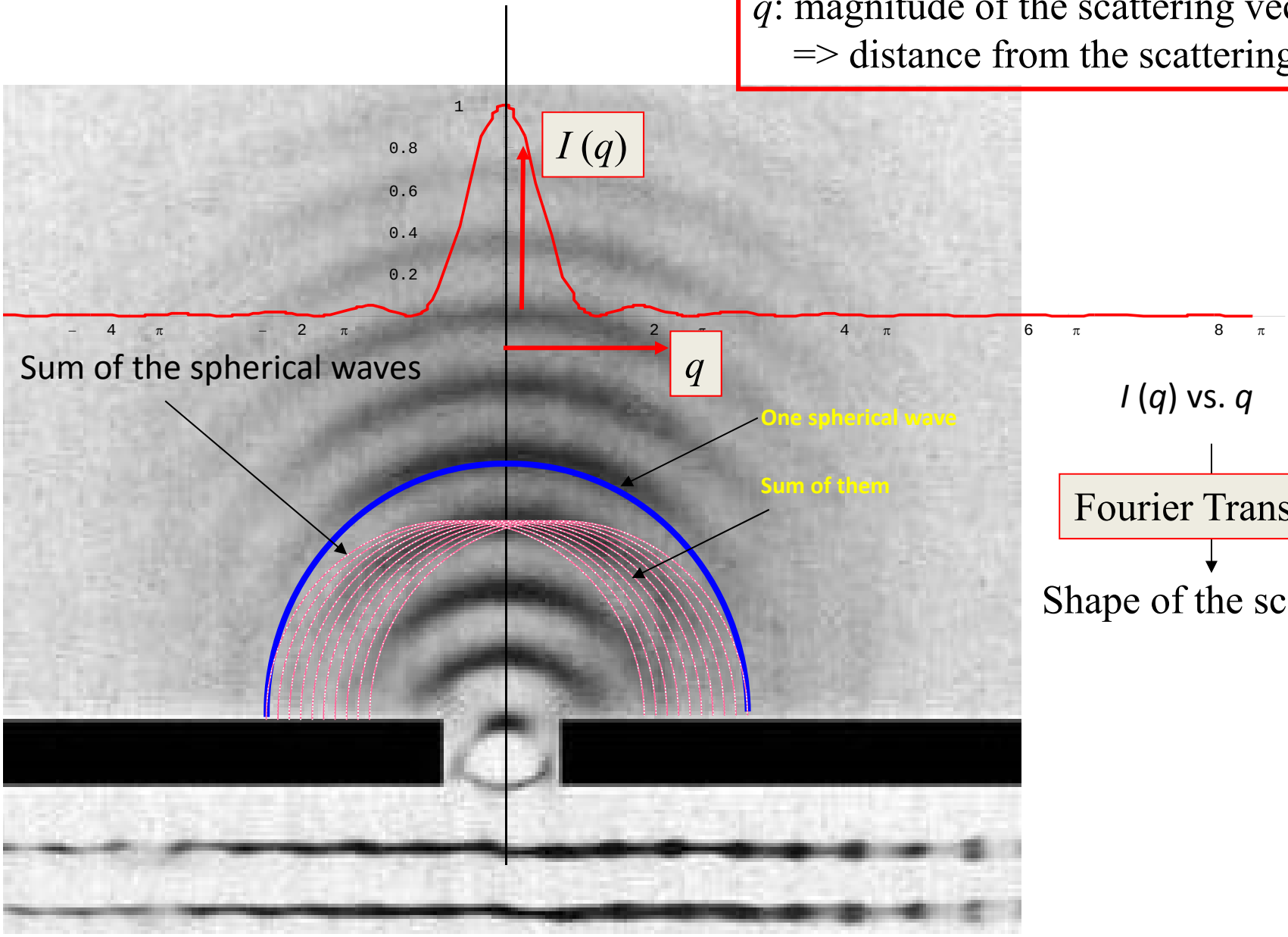

$I(q)$ vs. q

Fourier Transform

Shape of the scattering

SAXS at SPring-8 and our set-up

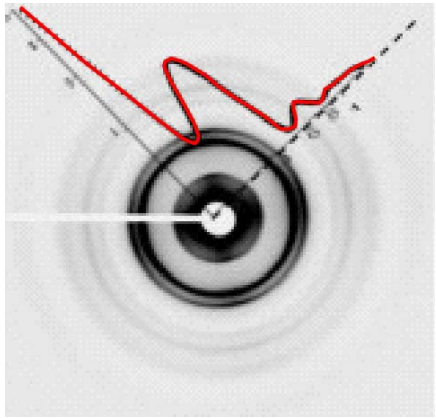

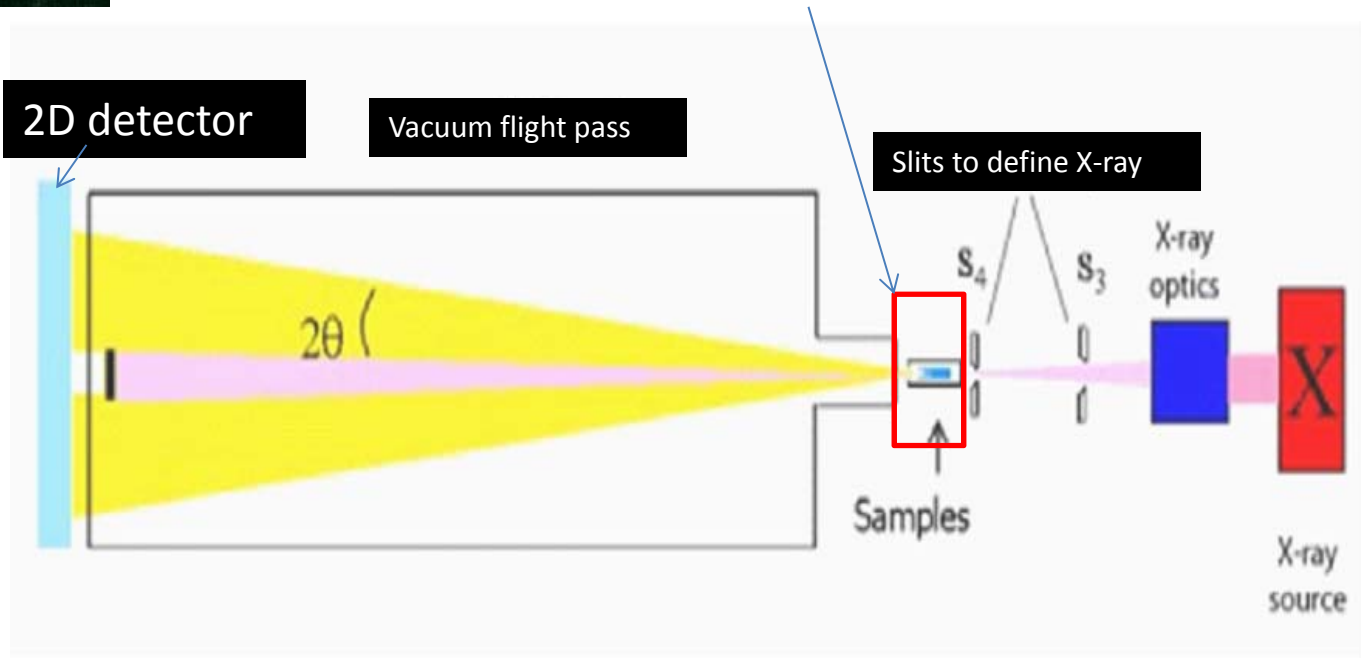

Scattering angle < 2 degree => 1 – 100 nm
Small angle X-ray scattering (SAXS)

$$q = \frac{2\pi}{\lambda}\sin\theta \qquad d \propto \frac{1}{q}$$

Determining the structure of matter

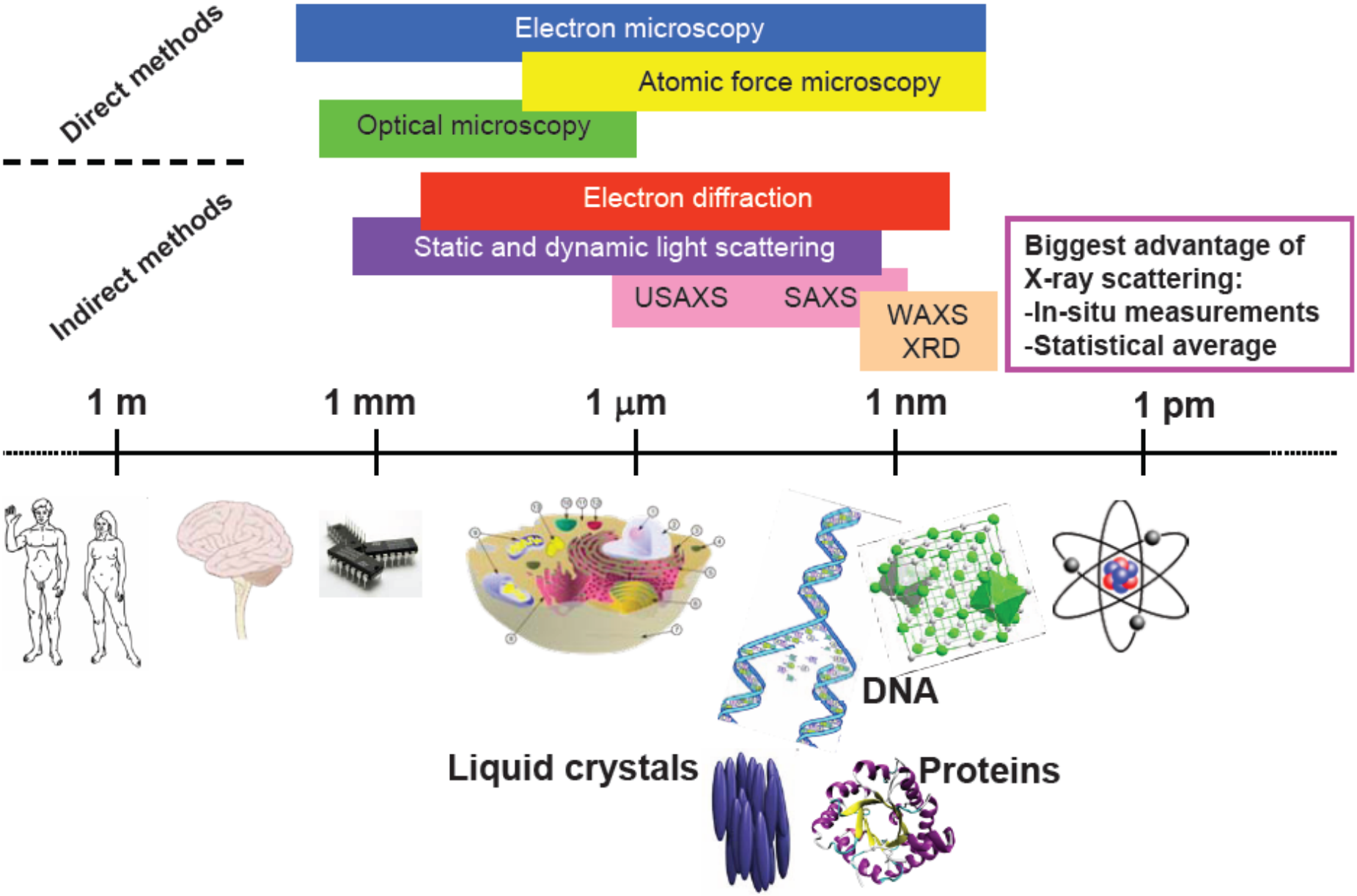

SAXSは5nmと10nmを峻別できる

区別ではなく、識別でなく、厳密に峻別できる

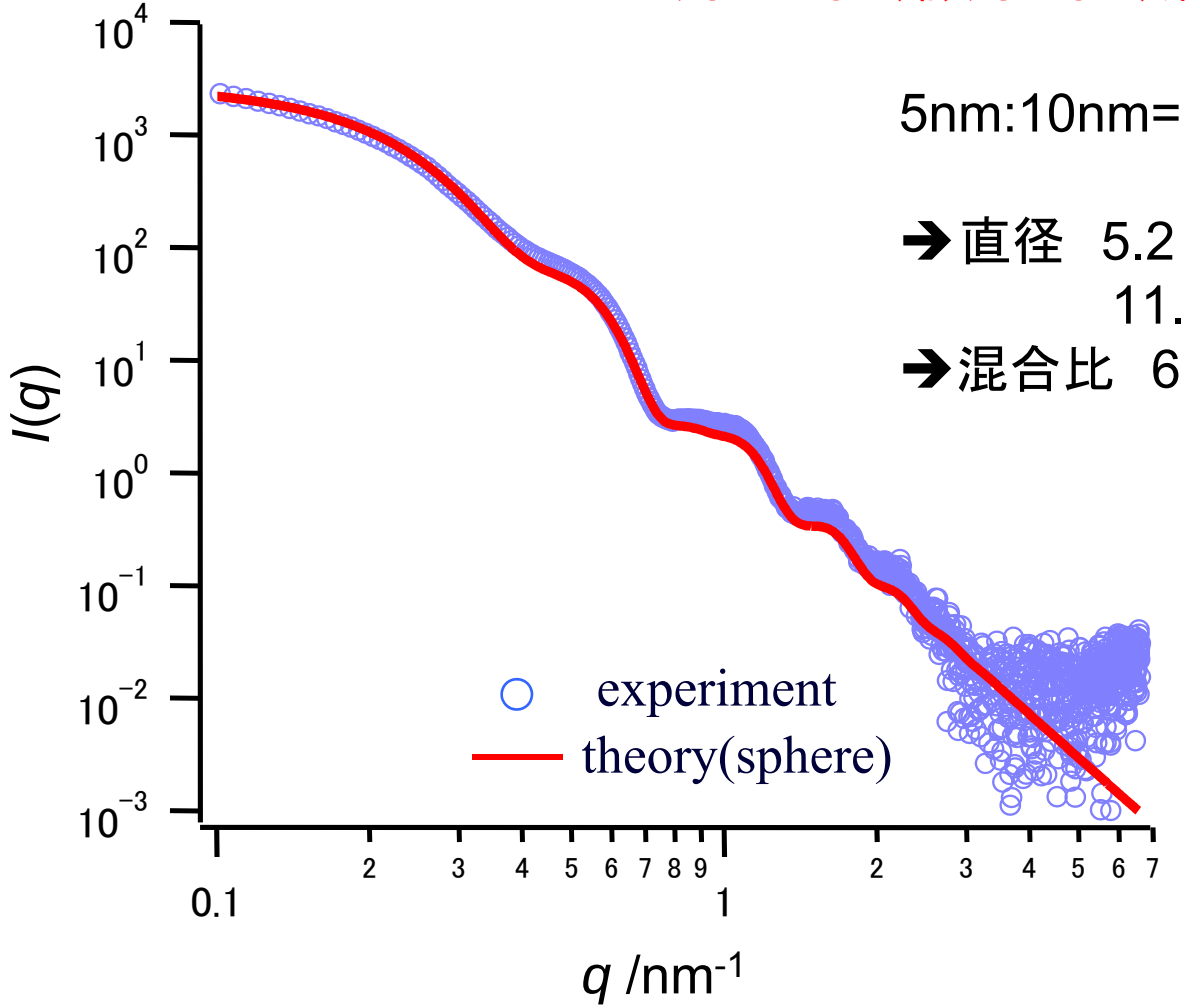

5nm:10nm=1:1混合

➔直径　5.2 ±0.1nm
　　11.3 ±0.2 nm

➔混合比　6.2:3.8 （個数比）

Outline

Self-assembly and Drug Delivery System (DDS)

Strength of SAS technique in exploring DDS particles

Examples from Our Recent Studies

- Polymeric Micelle for Delivering Hydrophobic Drugs

J. Am. Chem. Soc., 135 (7), 2574–2582(2013)
Macromolecules, (Web): July 23, (2012)
J. Phys. Chem. B, 8241–8250, (2012)
Polymer Journal, 44, 240-244 (2012)

- Monodisperse Calixarene Micelles for DNA Delivery

Langmuir, *28* (6), 3092–3101, (2012)
Bull. Chem. Soc. Jpn. 354-359 (2012)
Langmuir, 29 (45), 13666–13675,（2013）
Chem. Commun., 49, 3052-3054,（2013）

- Short DNA DDS for Immune-stimulation and Gene Silencing

J. Phys. Chem. B,, *116* (1), 87–94 (2012)
Molecular Therapy (Nature), 20, 1234-1241 (2012)
Journal of Controlled Release, 155-161 (2011)
Bioconjugate Chemistry 22 9-15, (2011)
J. Am. Chem. Soc. 126, 8372-8373, (2004)

Case 1: Polymeric Micelles

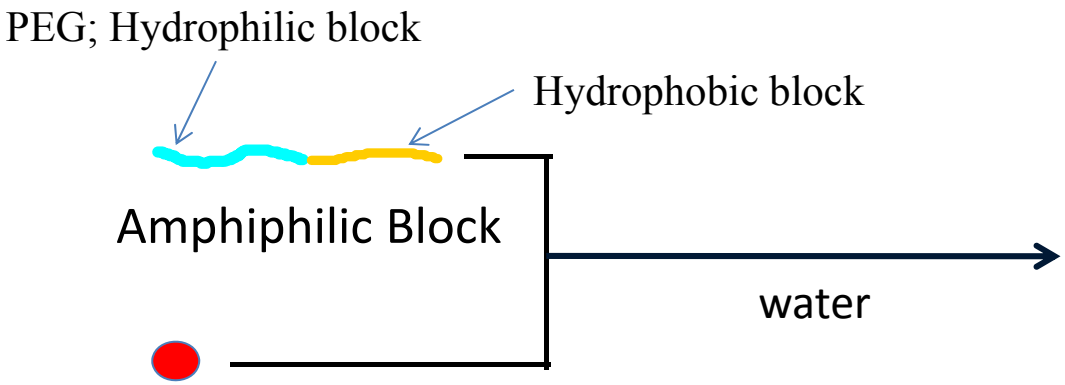

Hydrophobic drug (or equivalent Br-modified)

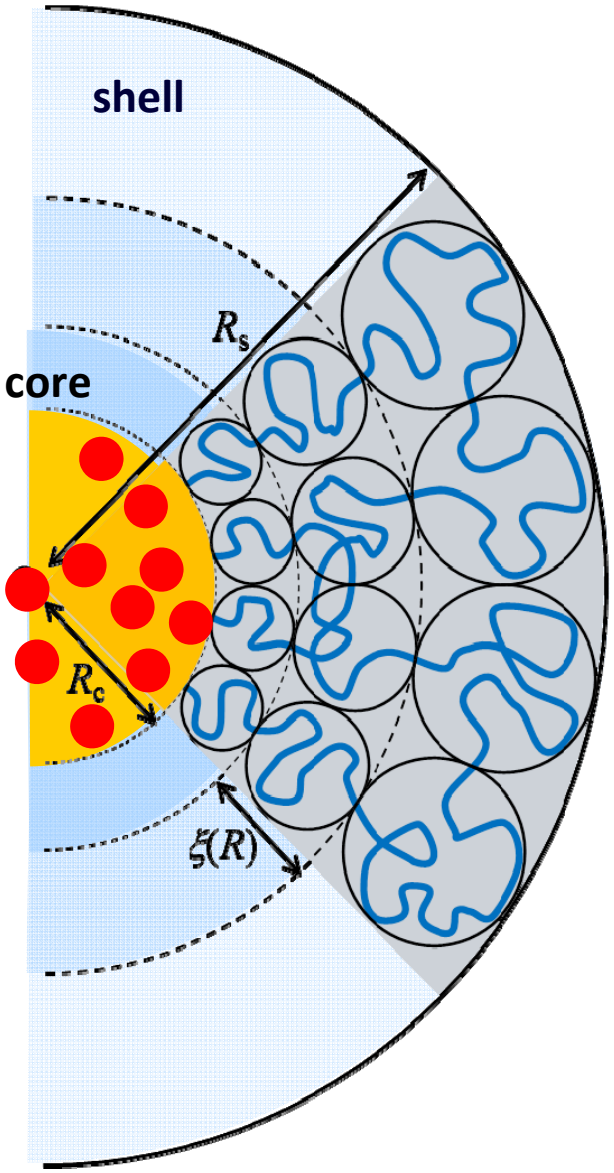

SAXS+FFF/MALS

➔ Aggregation number

➔ Core and corona sizes

➔ Nature of the interface: Overcrowding of PEG

ASAXS (anomalous SAXS)

➔ How the drugs are encapsulated in the core

➔ Difficult for normal SAXS

➔ Br attached molecule as a probe

FFF: filed flow fluctuation, MALS: multi-angle light scattering

Materials

poly(ethylene glycol)-*block*-poly(α,β-benzyl-*L*-aspartate) (PEG-PBLA)

Hydrophilic ;PEG

Hydrophobic Asparate

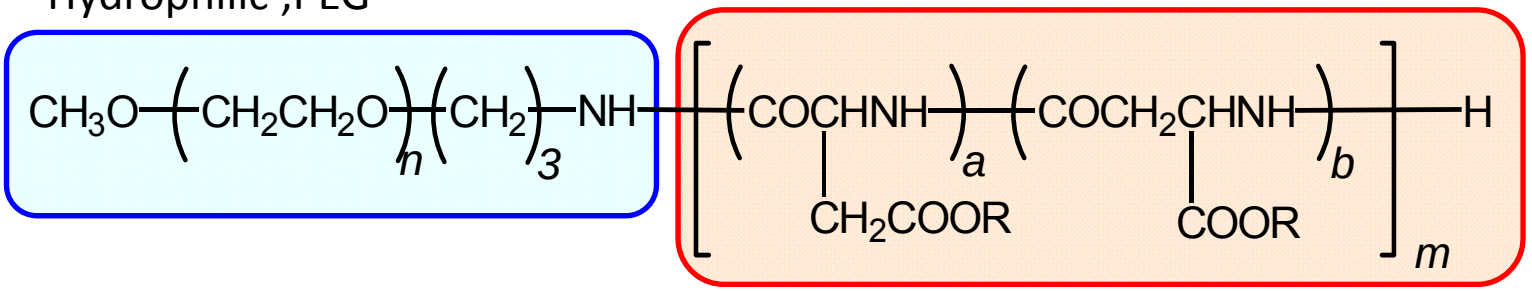

PEG

Asp

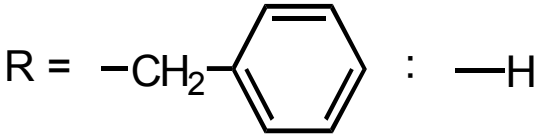

a: *b* = 3: 1

n of PEG = 118,
M_w = 5800

n of Asp = 20 – 30,
Benzylation ratio 60-90

n of PEG >> n of Asp → Stable Spherical micelle

SLS *vs.* SAXS from dilute solutions

$$I(\theta) = \frac{M_W}{N_A} C_M \bar{\nu}^2 (\bar{\rho} - \rho_0)^2 F(\theta)$$

M_W : weight average molecular weight

$\bar{\nu}$: partial specfic volume

$\bar{\rho} - \rho_0$: electron density difference between solvent and solute

$F(\theta) \rightarrow 1$ at low θ and low concentration

SLS (static light scattering) or MALS (multi-angles light scattering)

- $\bar{\nu}^2 (\bar{\rho} - \rho_0)^2$ can be determined as $\partial n / \partial c$, thus M_W can be evaluated .
- From $F(\theta)$, the radius of gyration ($< S^2 >$ or R_g) is determined.
- Can be coupled with GPC or FFF.

SAXS (small angle X-ray scattering)

- $\bar{\nu}^2$ and $(\bar{\rho} - \rho_0)^2$ should be determined separately and thus M_W cannot be determined.
- From $F(\theta)$, inner structures can be evaluated.

Molecular Characters

code	Asp number	Benzylation / %
HH9-31-1	26.4	76.9
HH9-31-2	26.4	81.4
HH9-24-2	26.4	88.6 (highest)
HH9-22-2	20.2 (shortest)	83.7
HH9-22-4	23.8	84.0
HH9-22-3	29.7	82.2
HH9-22-5	32.0 (longest)	77.2
HH9-24-1	26.9	65.8 (lowest)
HH9-18-1	26.9	83.3
HH9-32*	26.9	83.3

Benzylation

$$= \frac{\text{◯}}{[\text{COOH}] + \text{◯}}$$

Film was sonicated in PBS

* Dialysis

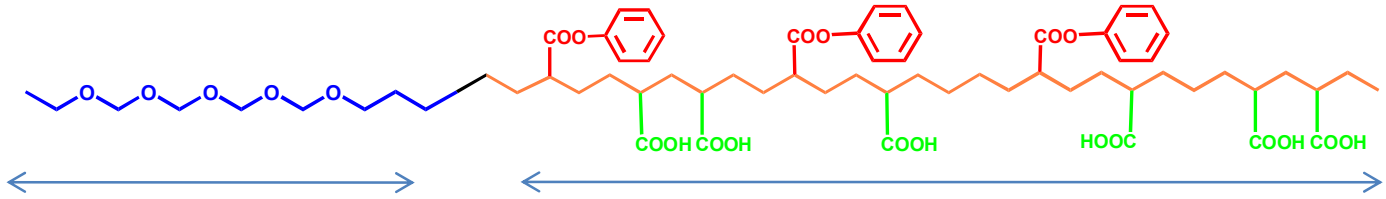

$\alpha/\beta=1/3$

M_w = 5.2 x 10^3
n = 118
M_w/M_n <1.05

Number of *Asp* = 20 - 30

From NMR

FFF coupled with MALS

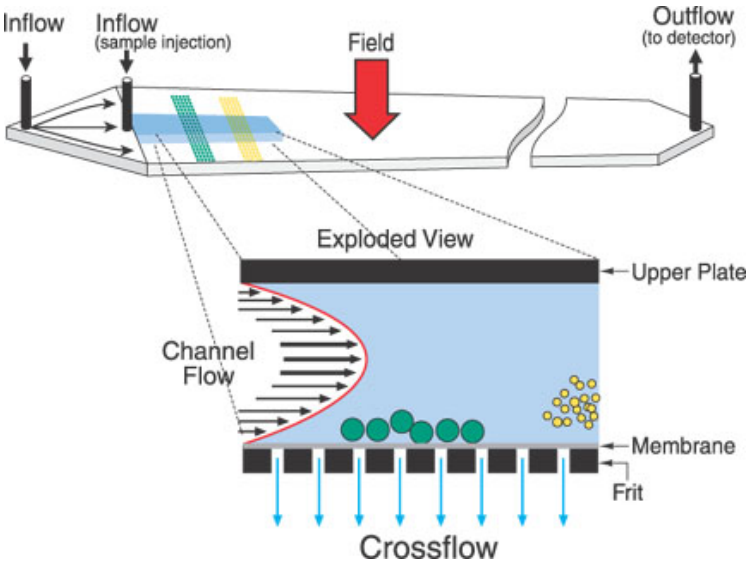

Field –Flow Fractionation

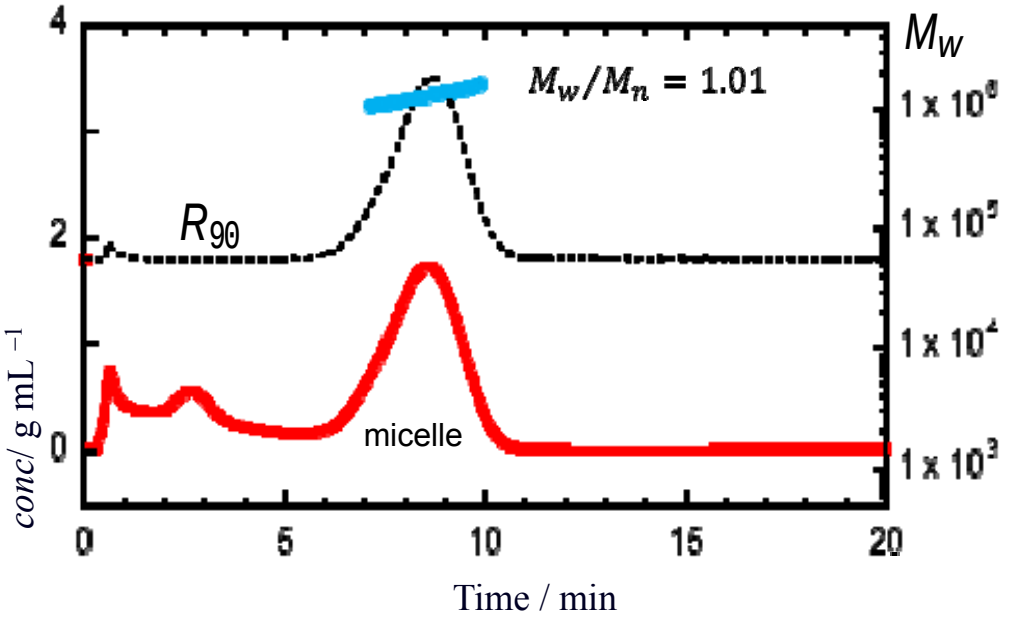

$$\left(KC/R_\theta\right)_{c\to 0}^{1/2} = \frac{1}{M^{1/2}} + \frac{1}{6}\frac{<S^2>}{M^{1/2}}k^2 + O\left(k^4\right)$$

$$K = \frac{4\pi^2 n_0^{\,2}\left(dn/dc\right)^2}{N_A \lambda_0^{\,4}}$$

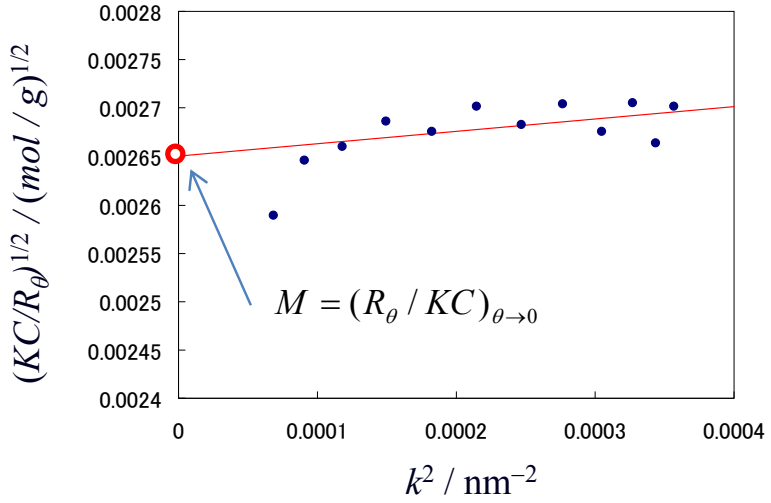

What determines the aggregation number ?

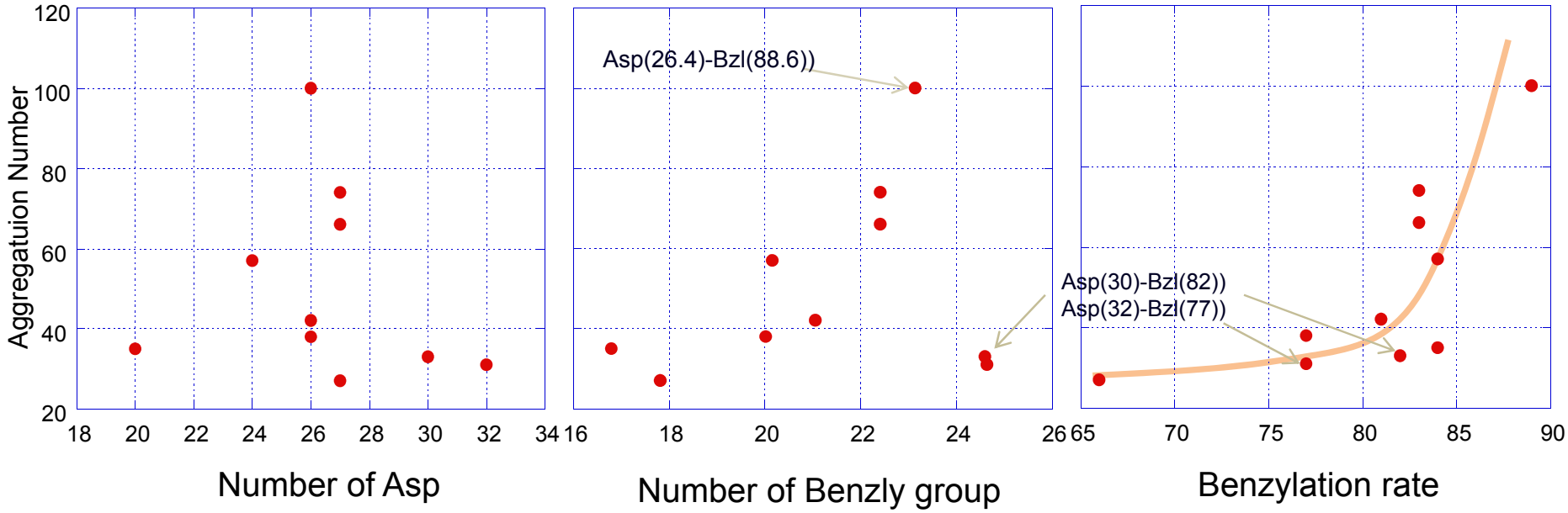

$$N_{agg} = \frac{Mw \text{ for micelle}}{Mw \text{ for one block}}$$

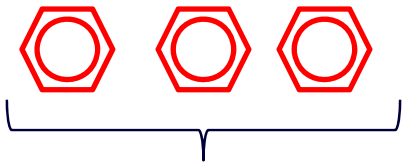

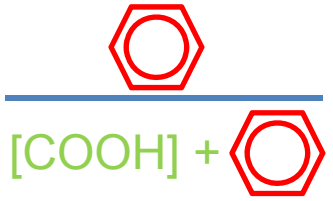

➔ Hydrophobic nature is the major factor

SAXS from a PEG-Asp/Bzl micelle

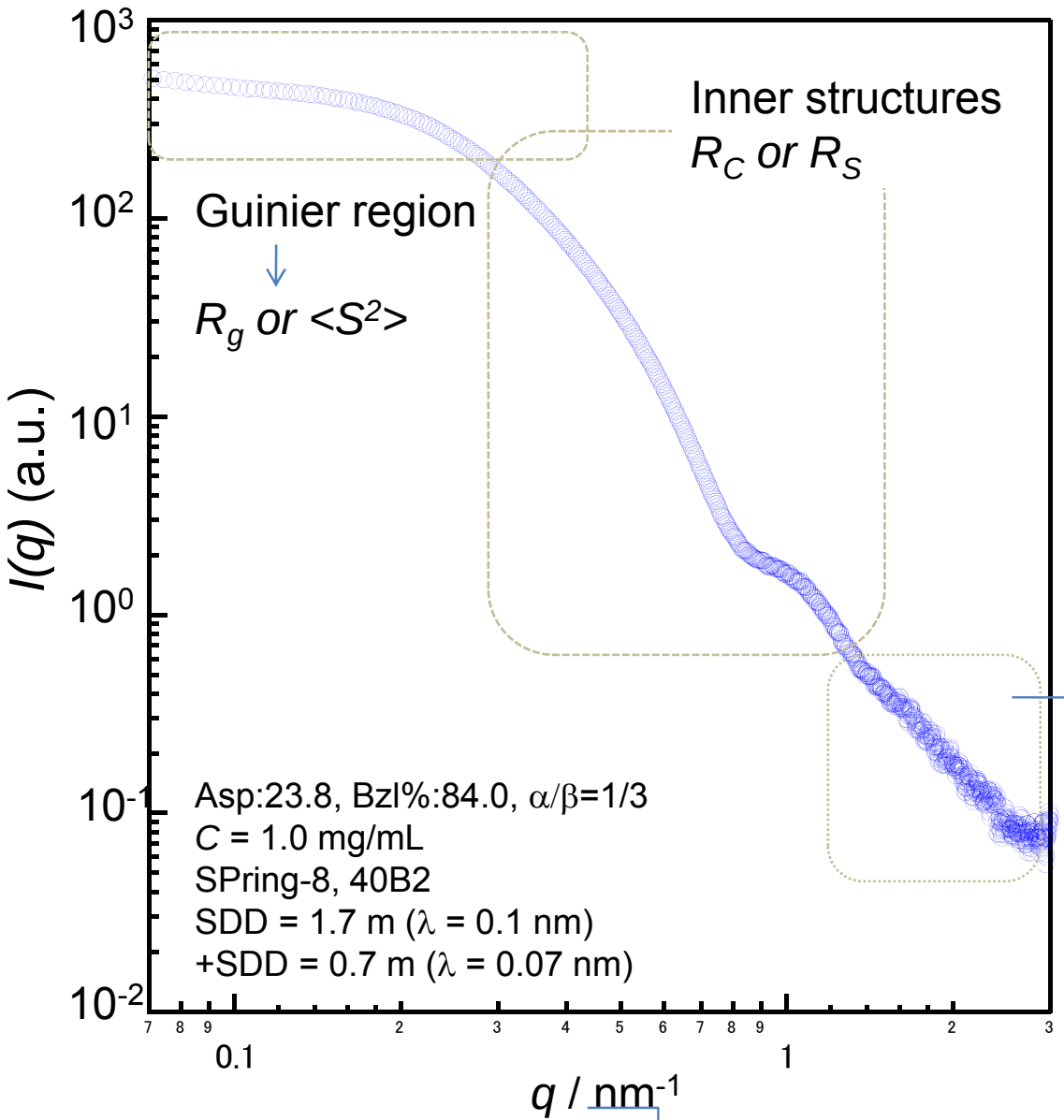

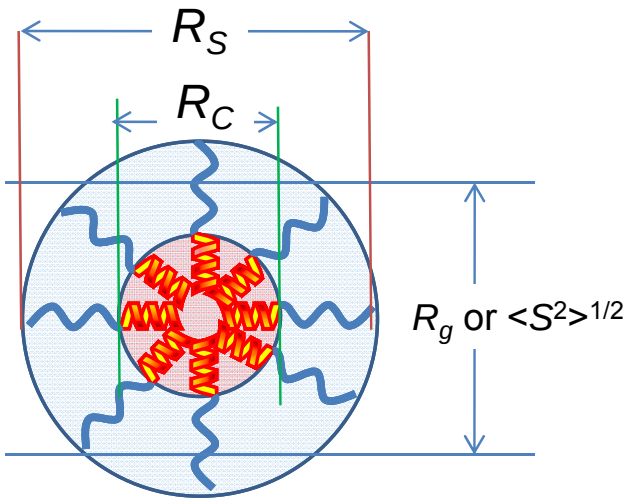

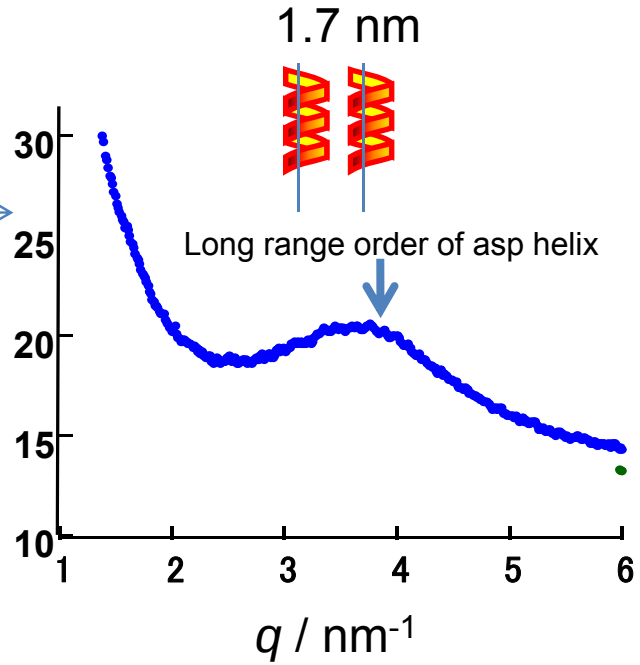

Optical impurities in LS and SAXS

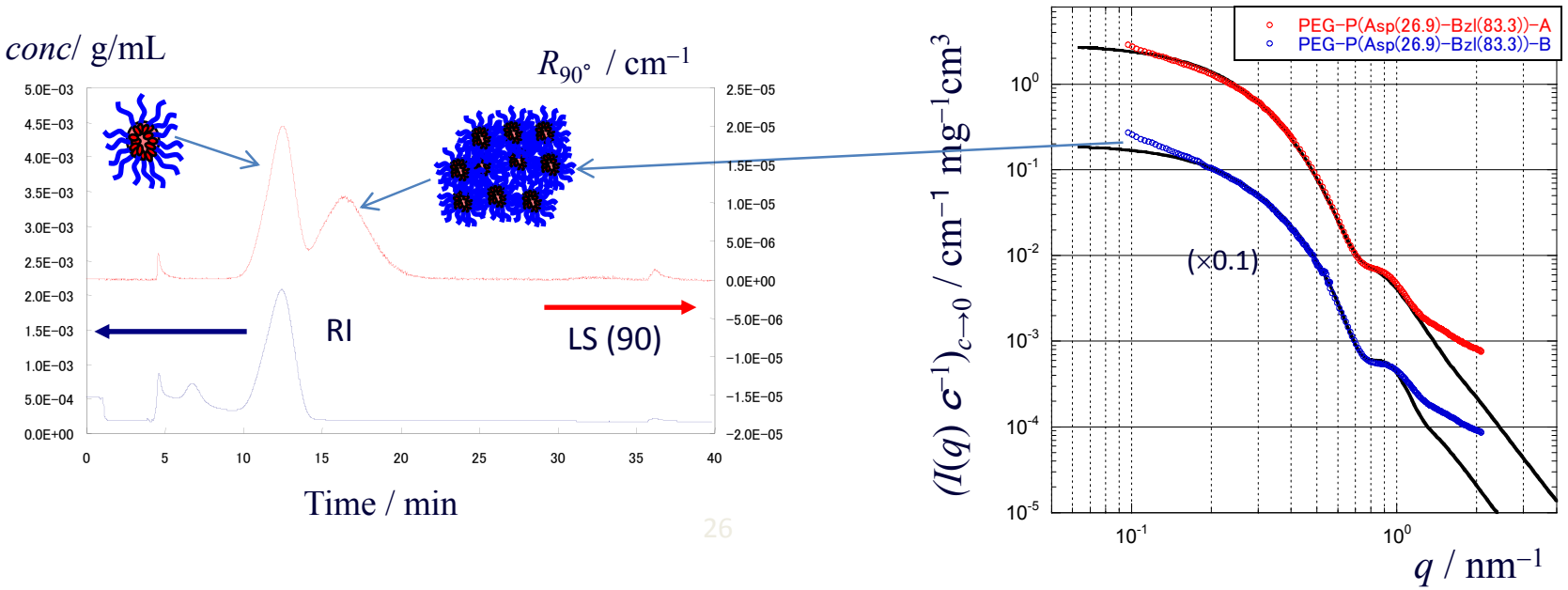

LS ➔ impossible to obtain accurate Mw in batch measurement

Fitting Model for SAXS

$$I(q) = P(R_s)\cdot N\left\{(\rho_c-\rho_s)V_c\frac{3\left[\sin(qR_c)-qR_c\cos(qR_c)\right]}{(qR_c)^3}+(\rho_s-\rho_0)V_s\frac{3\left[\sin(qR_s)-qR_s\cos(qR_s)\right]}{(qR_s)^3}\right\}^2$$

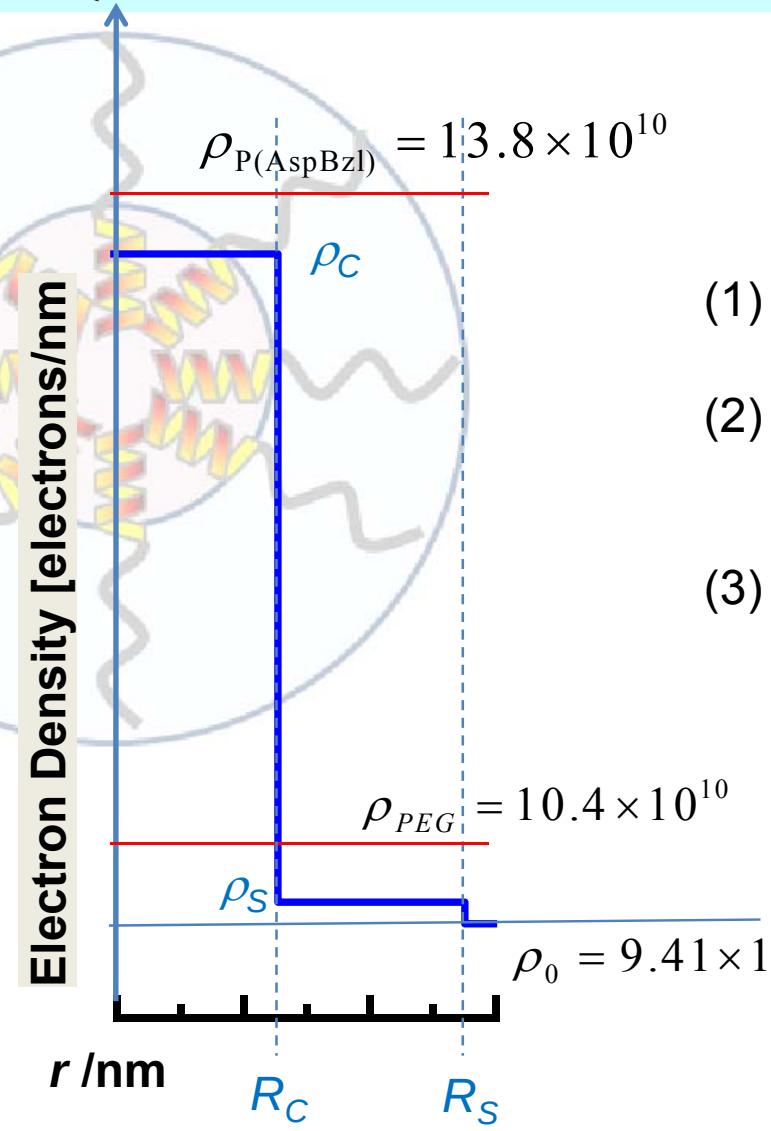

Fitting parameters: R_S, R_C, ρ_C, ρ_S

Given values: N, ρ_0 → LS

(1) Absolute X-ray intensity calibrated with water and PEG.

(2) Extrapolation

$$\left(\frac{I(q)}{c}\right)_{c=0} = \lim_{c\to0}\frac{I(q)}{c}$$

(3) To fit the data assuming the distribution in the core size

$$P(R) = \frac{1}{V}\cdot\frac{1}{\sqrt{2\pi}\sigma}\exp\left[-\frac{(R-R_0)^2}{2\sigma^2}\right]$$

and $\rho_0 < \rho_S < \rho_{PEG}$, & $\rho_C < \rho_{P(AspBzl)}$

SAXS from a PEG-Asp/Bzl micelle

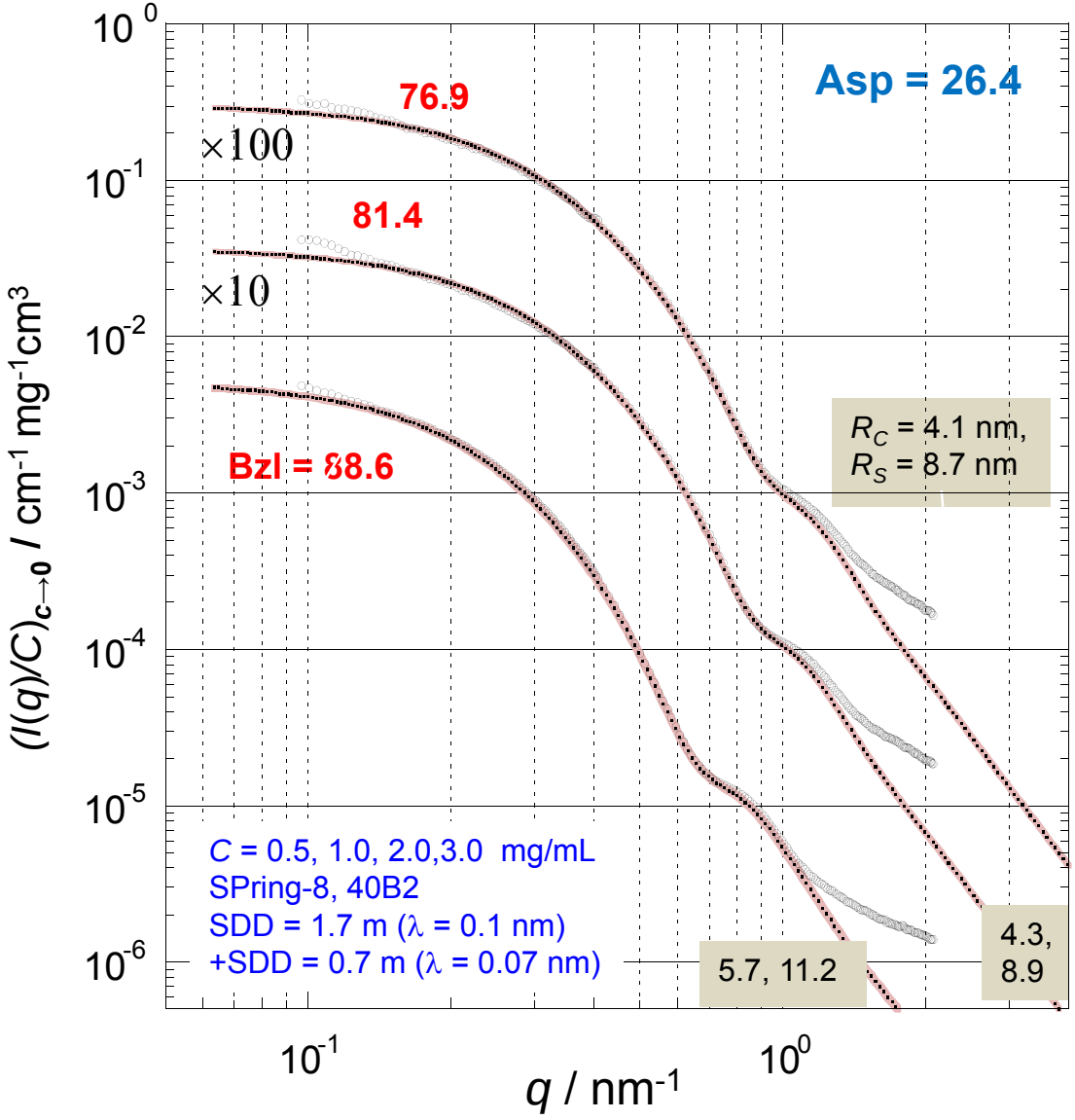

Sanada et al., *J. Phy. Chem. B* (2012)

Fitting model: Core-corona model
Pedersen et al., *Macromolecules* 2003.

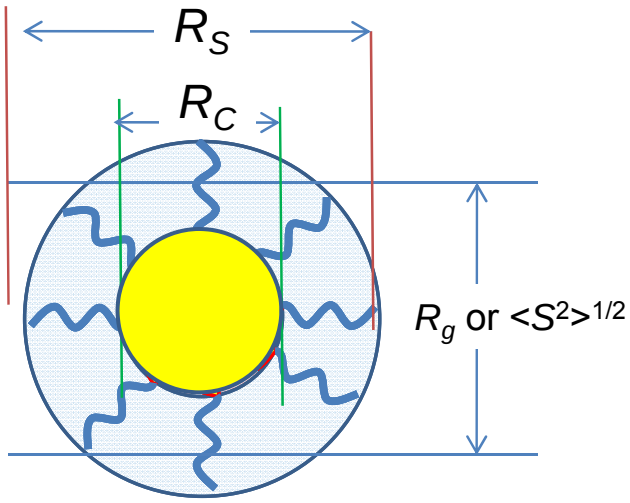

The secondary factor: the Asp length

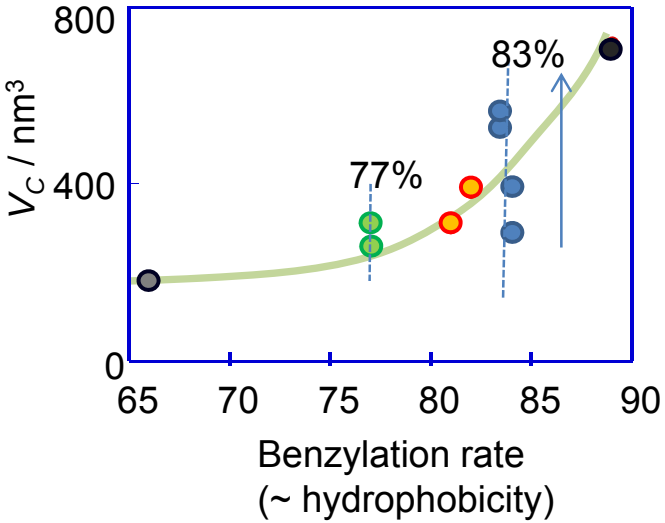

Scaling Theory of the Spherical Micelles

$$G = G_{core}(R_e, \varphi) + G_{in}(\gamma) + G_{shell}(\chi)$$

G_{core} the entropic elasticity of the core chains determined by

$$R_e / R_C$$

G_{in} the interfacial tension between the core chains and the solvent molecules. γ increase with increase of the hydrophobicity of the core.

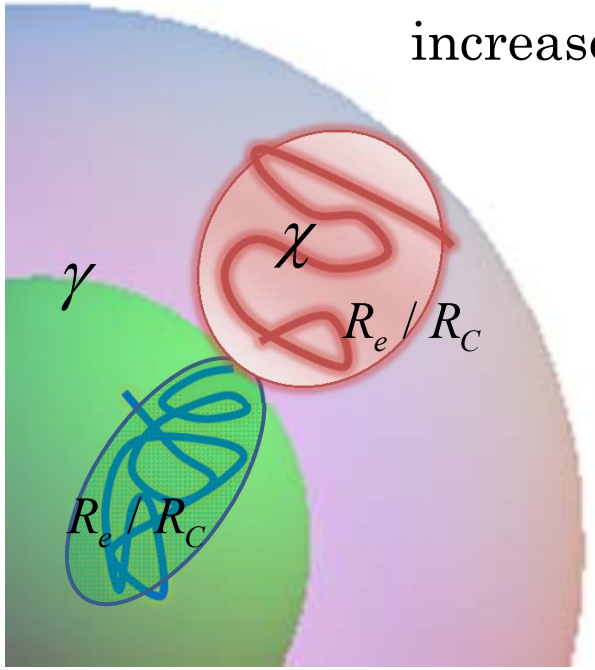

G_{shell} the osmotic energy: balance of the elastic stretching and the excluded volume effect.

The chain length dependence of the core size.

-Sailing theory tells the aggregation number is determined by the entropic packing of the core chains.
-No dependence of the shell chain.

Chain length of the core block

$$R_C \propto a_C \left(\frac{N_C}{\varphi} \right)^{3/5} \gamma^{2/5}$$

surface free energy per monomer, increased by three times for 83 and 77.

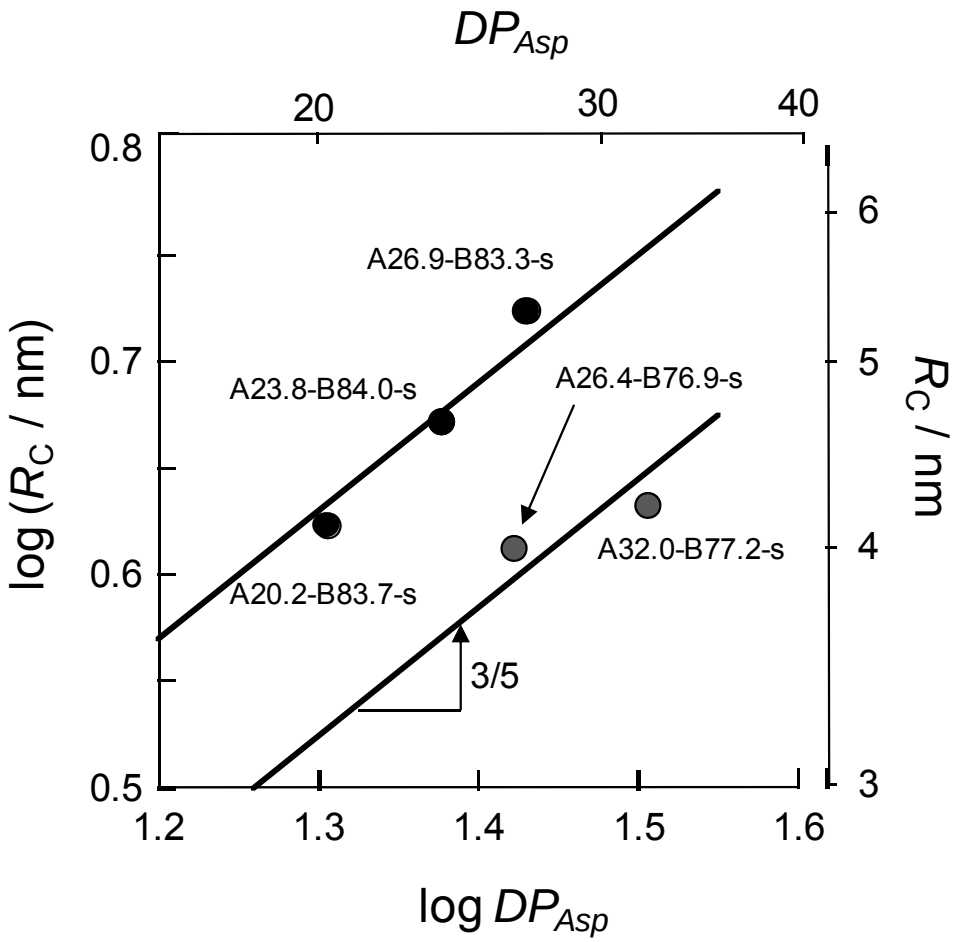

DP_{Asp} dependence of R_C for the same R_{Bzl}.

Scaling theory for polymeric micelles:
Zhulina *Macromolecules* **2005,** Halperin, A., *Macromolecules* **1987,** de Gennes, P. G., 1979.

Crowding Nature of the PEG chains in the Corona

The aggregation number and the core size
→PEG chain crowding

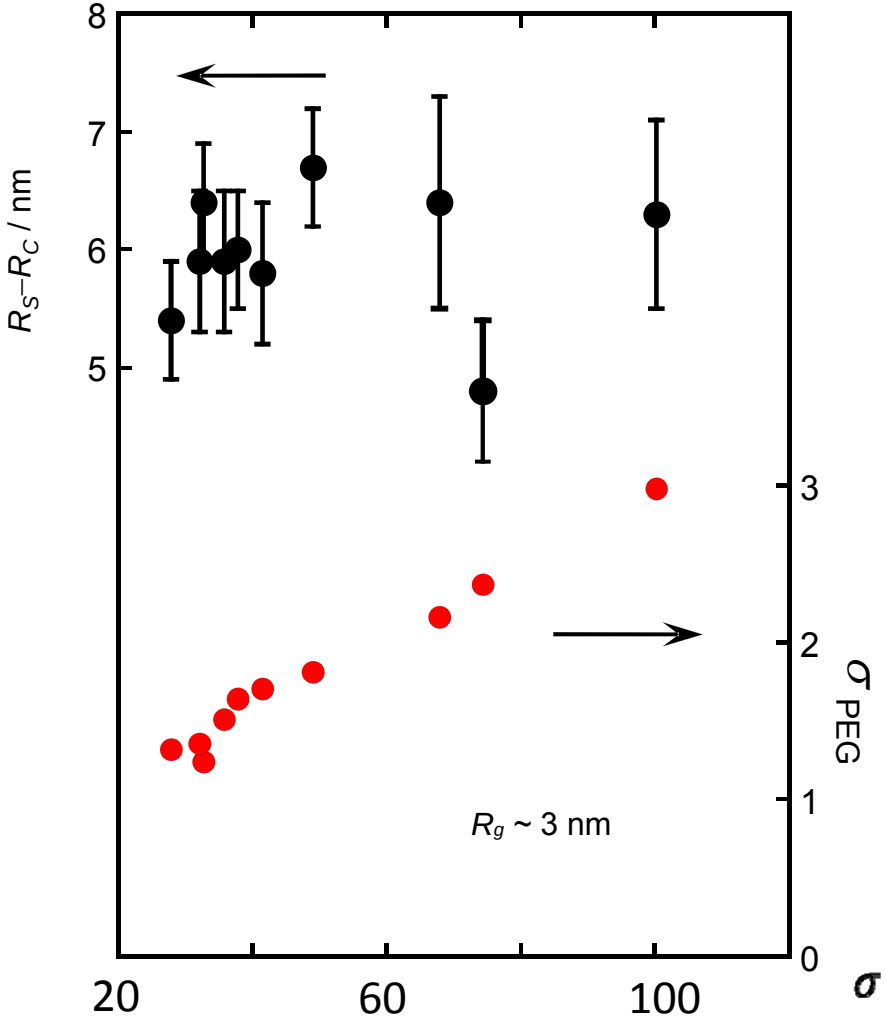

~ the benzylation rate~hydrophobicity

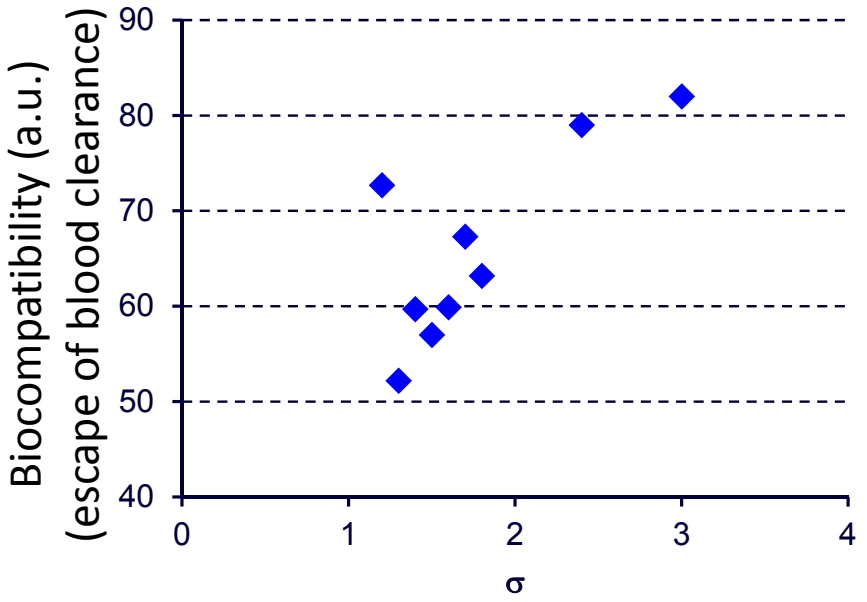

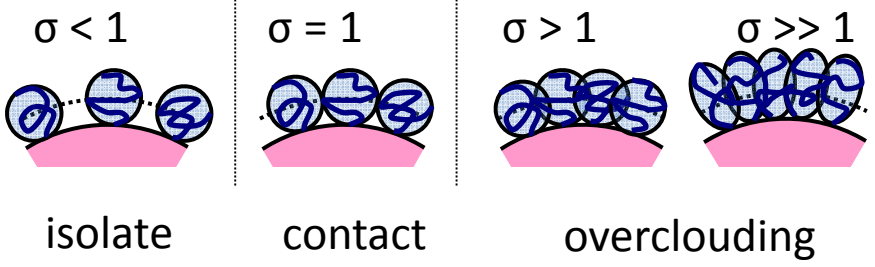

cross sectional area of free PEG

$$\sigma = \frac{\pi R_{g0}^2}{4\pi \left(R_C + R_{g0}\right)^2 / N_{agg}}$$

occupied area by one chain on the surface

PEG-Poly(Asp,Bzl) Micelle

Collaborating with Prof. Yokoyama
Jikei medical school

Di-Block Copolymer

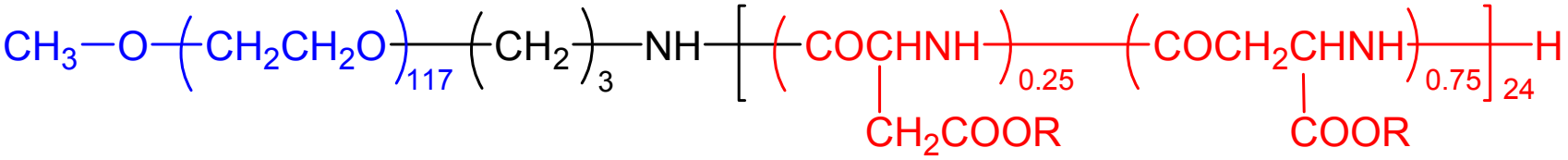

PEG—P(Asp Bzl)

R = H (27.4 %) or —CH2— (82.6 %)

Drug **LE540**

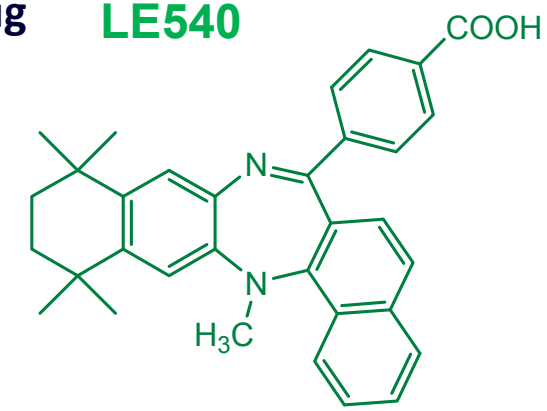

When the loading ratio exceeds 9-10 %,
LE starts leaking.
=> What is the inclusion mechanism ?

Neuroblastoma: Pre-incubation of SH-SY5Y human neuroblastoma cells with either RAR-pan-antagonist LE540 or MAP kinase kinase 1 (MEK-1) inhibitor PD98059.
Breast Neoplasms (Breast Cancer) In ZR-75-1 human breast cancer cells, cotreatment of LE135 and LE540 with all-trans-RA inhibited all-trans-RA-induced apoptosis.

SAXS from a PEG-Asp/Bzl micelle

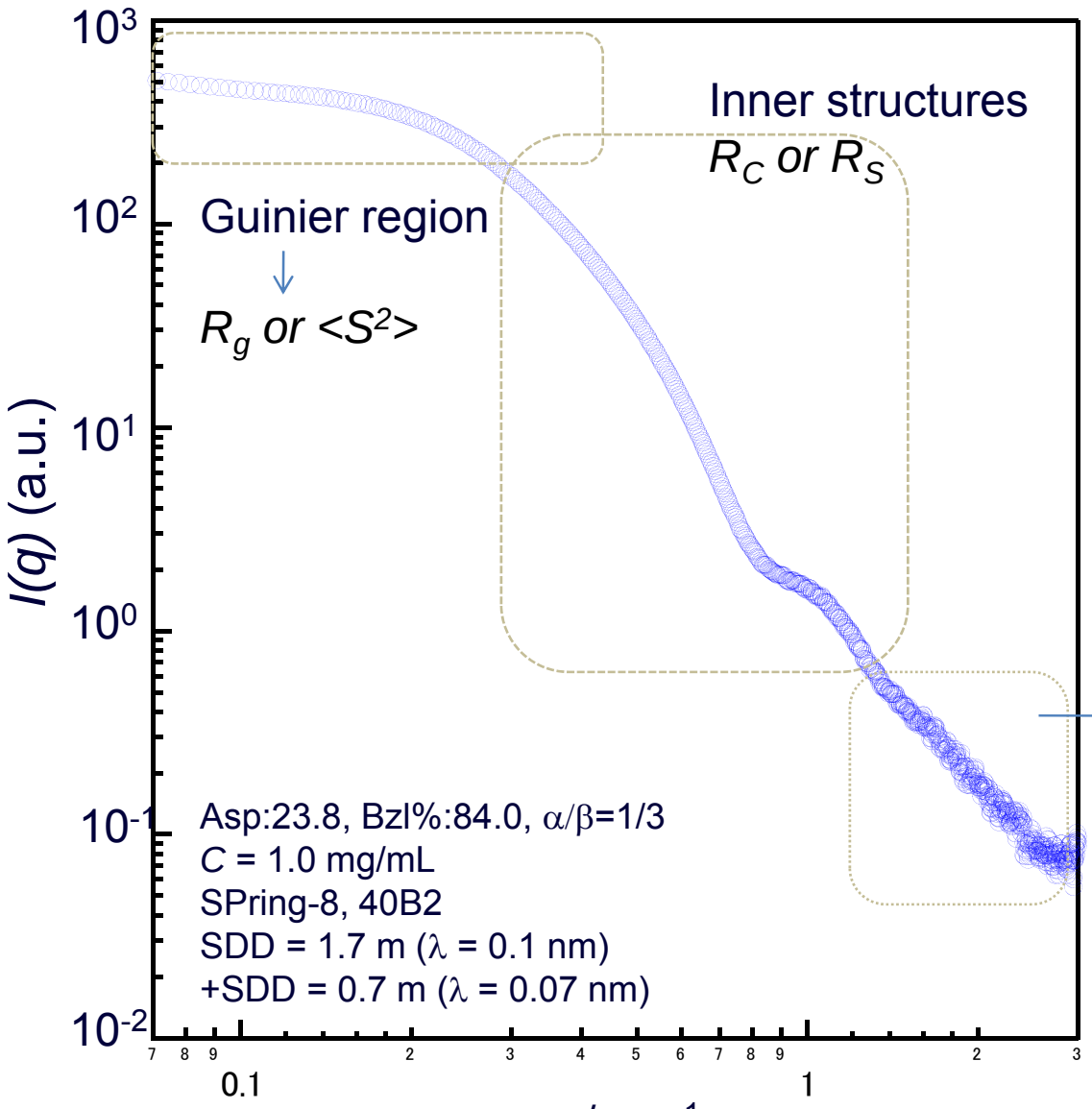

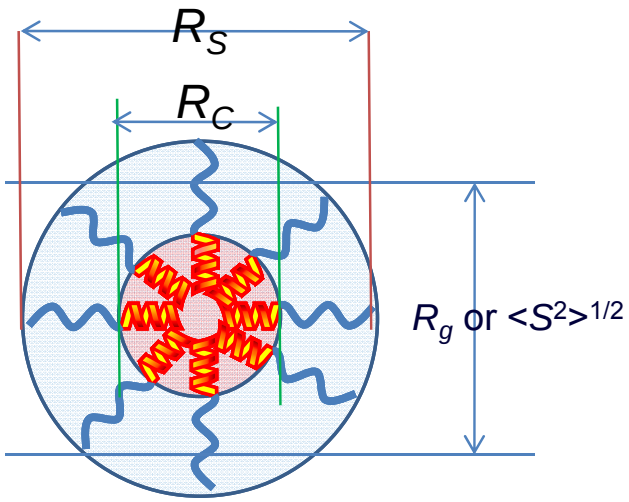

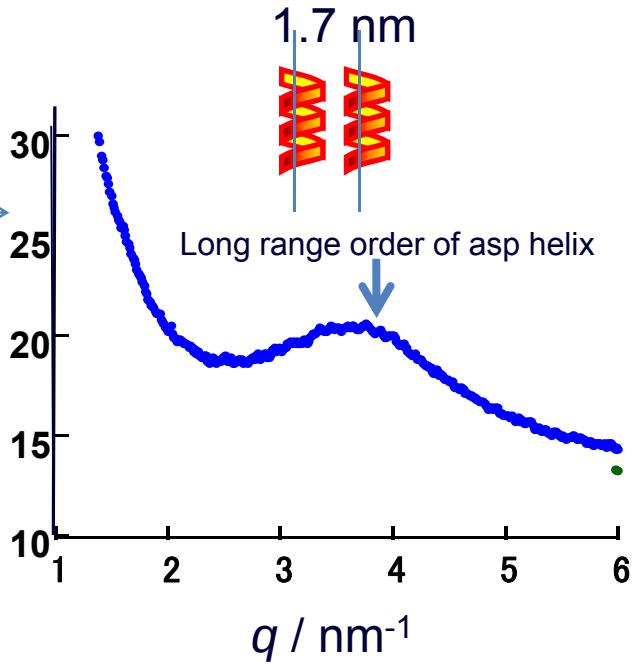

Related to diffraction angle

Density change upon loading

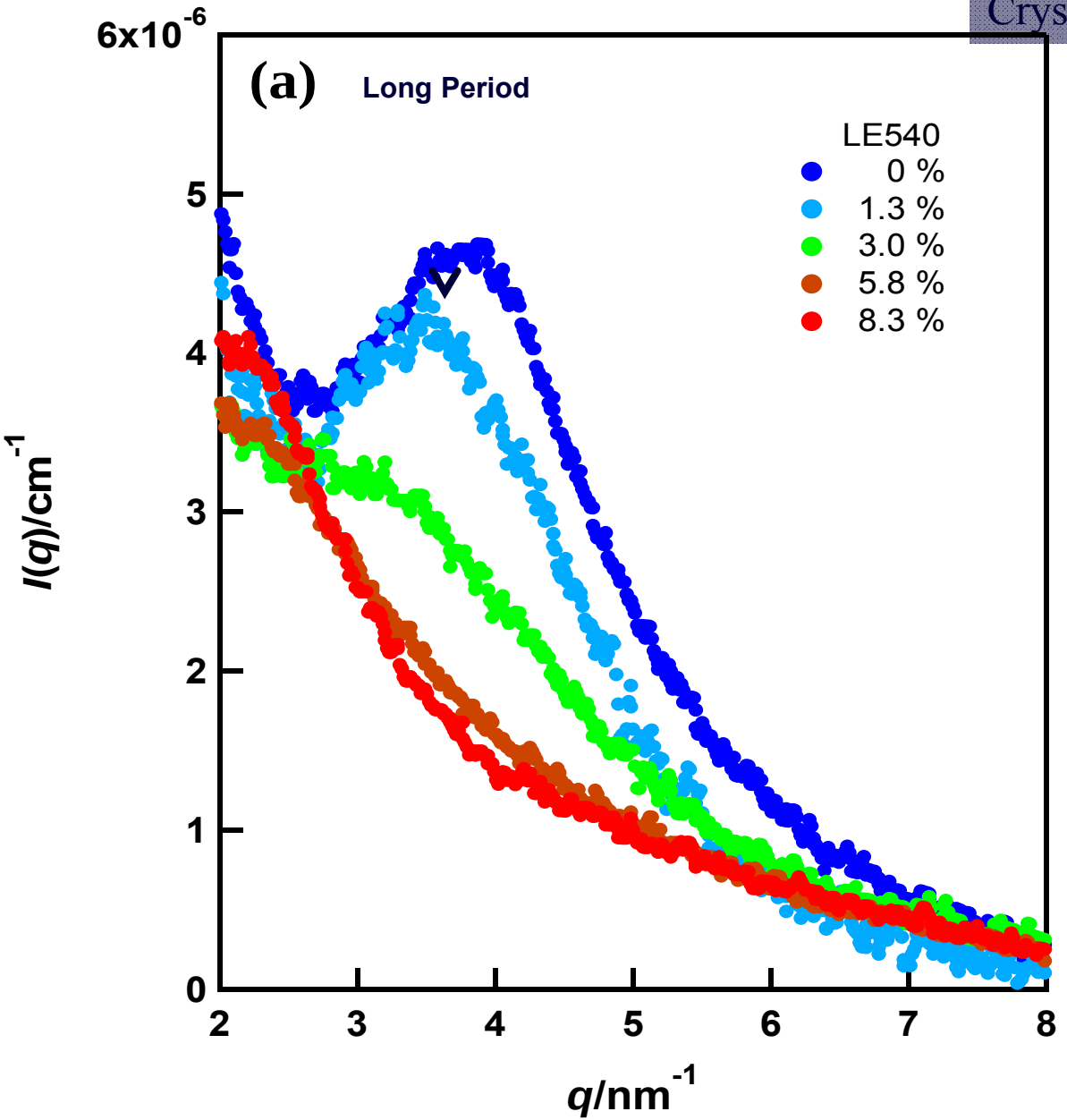

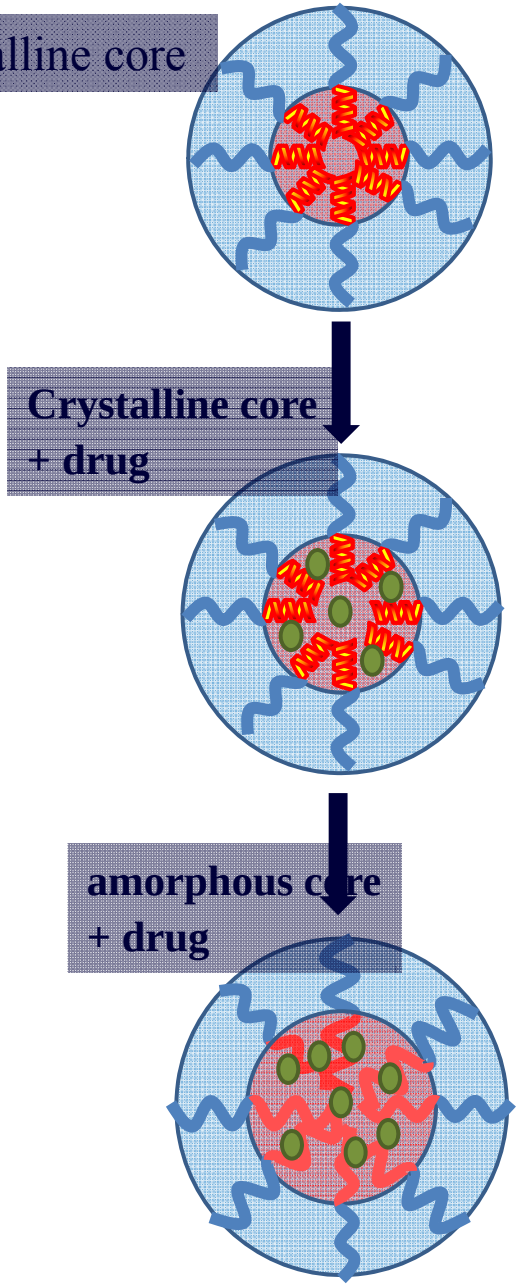

What's ASAXS ?

Anomalous Small-Angle X-ray Scattering　X線小角異常散乱

Resonance Small-Angle X-ray Scattering　X線小角共鳴散乱

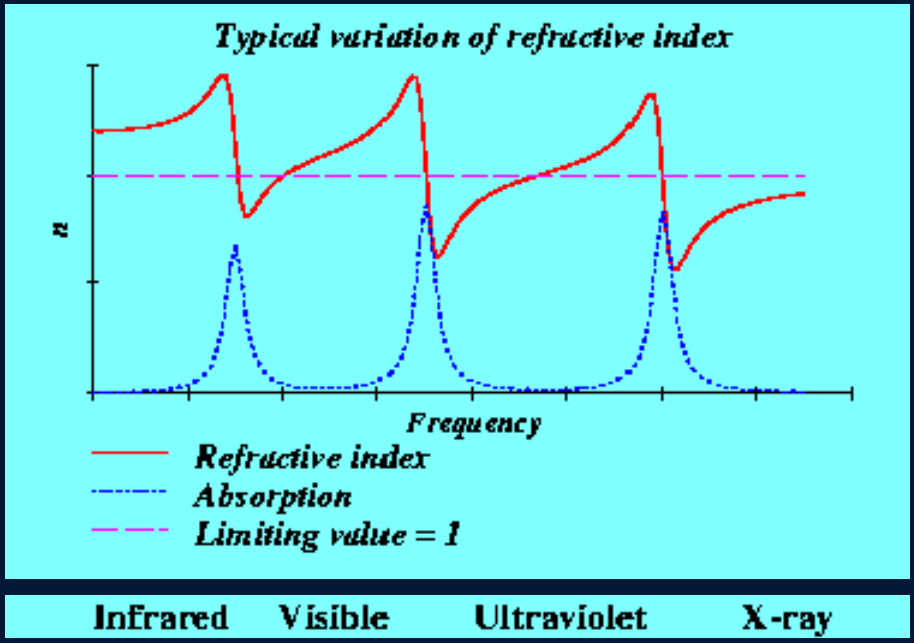

Reflective index

absorbance

Electron Adsorption Edge

	1	2	3	4	5	6	7	8	9	10	11	12	13	14	15	16	17	18
1						1 H												2 He
2	3 Li	4 Be											5 B	6 C	7 N	8 O	9 F	10 Ne
3	11 Na	12 Mg											13 Al	14 Si	15 P	16 S	17 Cl	18 Ar
4	19 K	20 Ca	21 Sc	22 Ti	23 V	24 Cr	25 Mn	26 Fe	27 Co	28 Ni	29 Cu	30 Zn	31 Ga	32 Ge	33 As	34 Se	35 Br	36 Kr
5	37 Rb	38 Sr	39 Y	40 Zr	41 Nb	42 Mo	43 Tc	44 Ru	45 Rh	46 Pd	47 Ag	48 Cd	49 In	50 Sn	51 Sb	52 Te	53 I	54 Xe
6	55 Cs	56 Ba		72 Hf	73 Ta	74 W	75 Re	76 Os	77 Ir	78 Pt	79 Au	80 Hg	81 Tl	82 Pb	83 Bi	84 Po	85 At	86 Rn
7	87 Fr	88 Ra		104 Du	105 Jo	106 Rf	107 Bh	108 Ha	109 Mt									

K-edge 5 keV- 20 keV

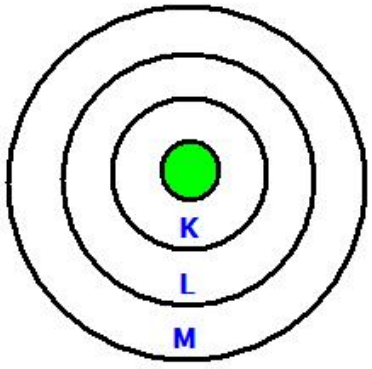

Bohr Atomic Model

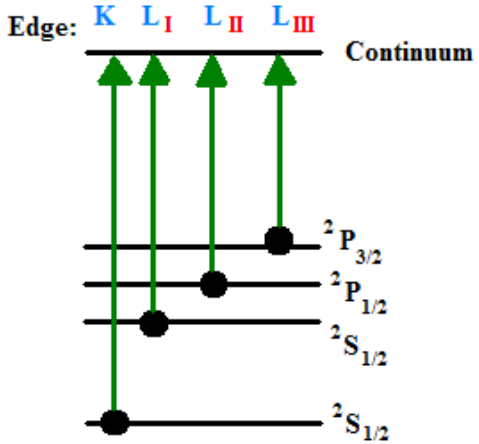

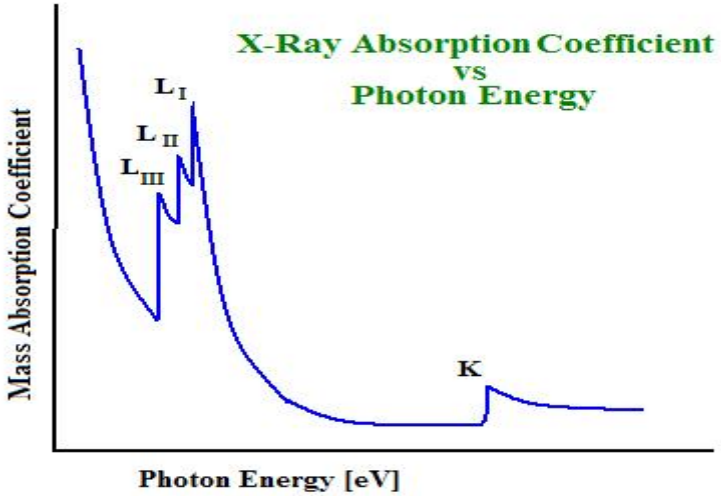

ASAXS Measurement

SAXS measurements were carried out with several X-ray energy near absorption edge.

From the difference of spectra of some X-ray energy, scattering property of specific atom can obtain.

$$I(q)_{Br} \propto C \times \left[\frac{I(q)_{E_1} - I(q)_{E_2}}{f'_{E_1} - f'_{E_2}} - \frac{I(q)_{E_1} - I(q)_{E_3}}{f'_{E_1} - f'_{E_3}} \right]$$

$$C = f'_{E_2} - f'_{E_3} + \frac{f''^{\,2}_{E_1} - f''^{\,2}_{E2}}{f'_{E_1} - f'_{E_2}} - \frac{f''^{\,2}_{E_1} - f''^{\,2}_{E3}}{f'_{E_1} - f'_{E_3}}$$

X-ray absorption edge of Br

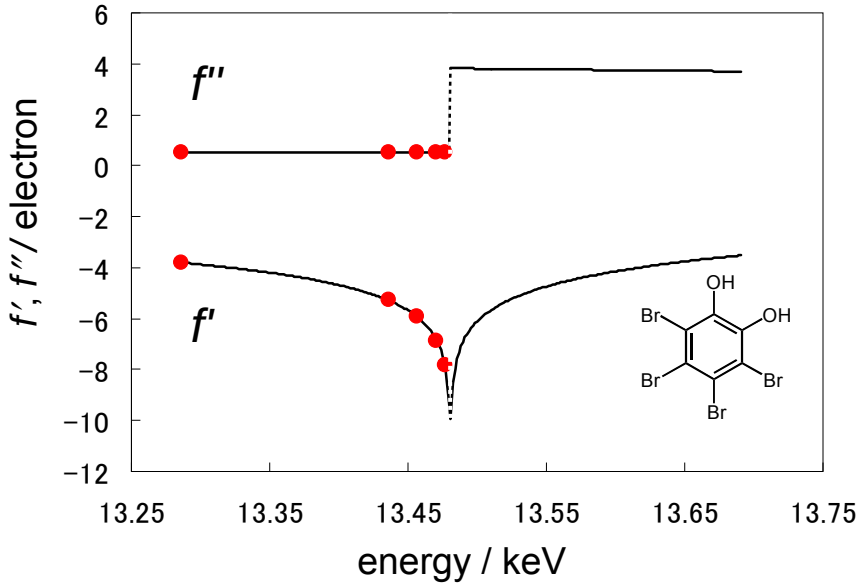

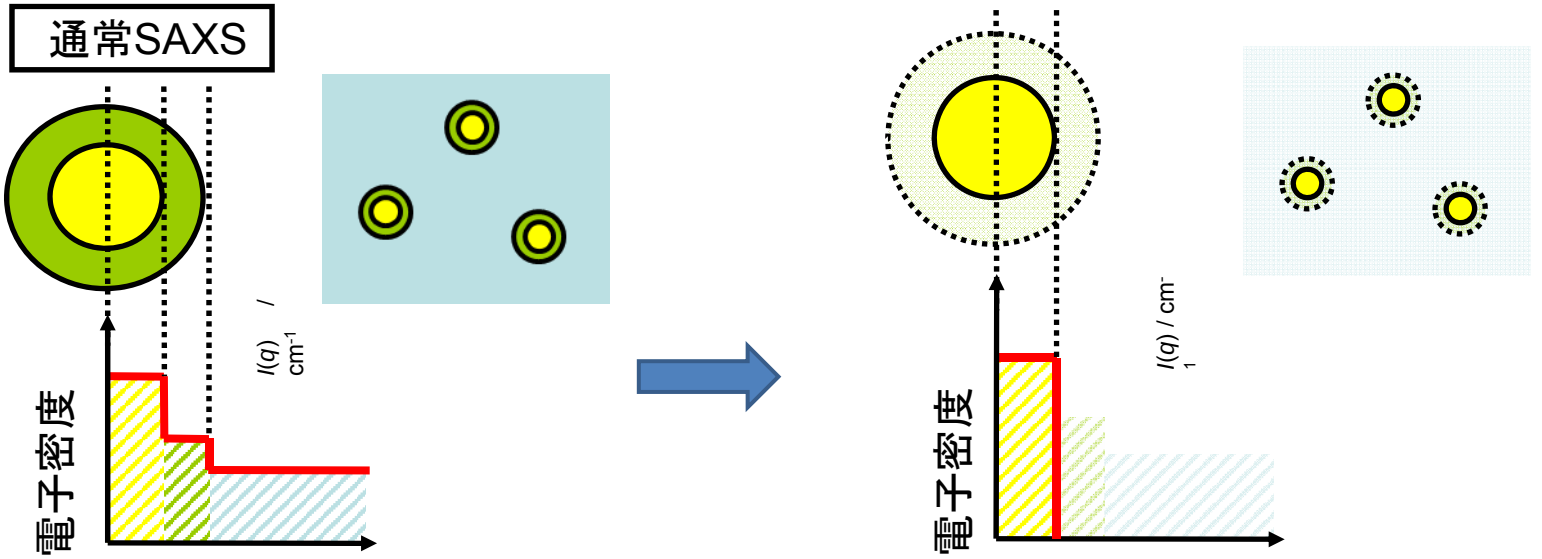

Increase S/N fro dilute solutions

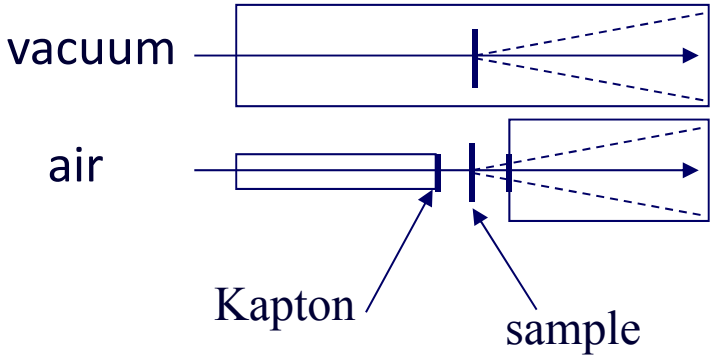

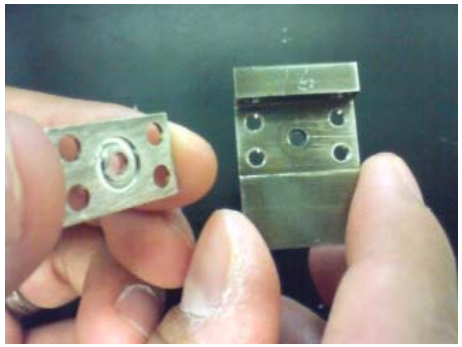

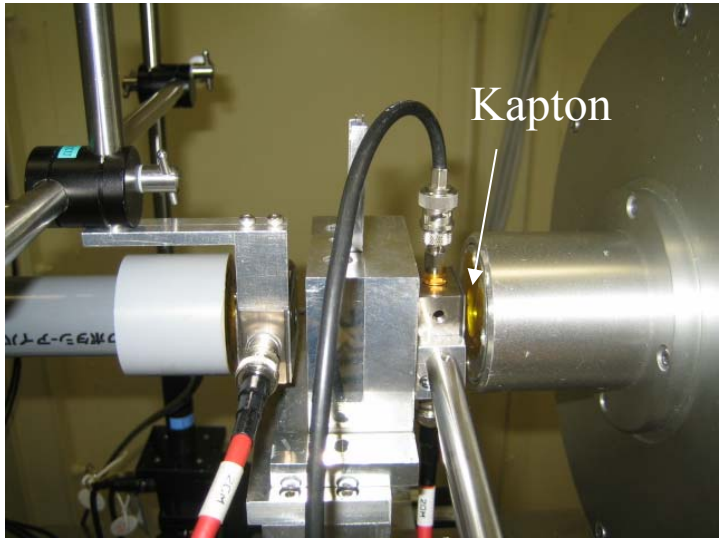

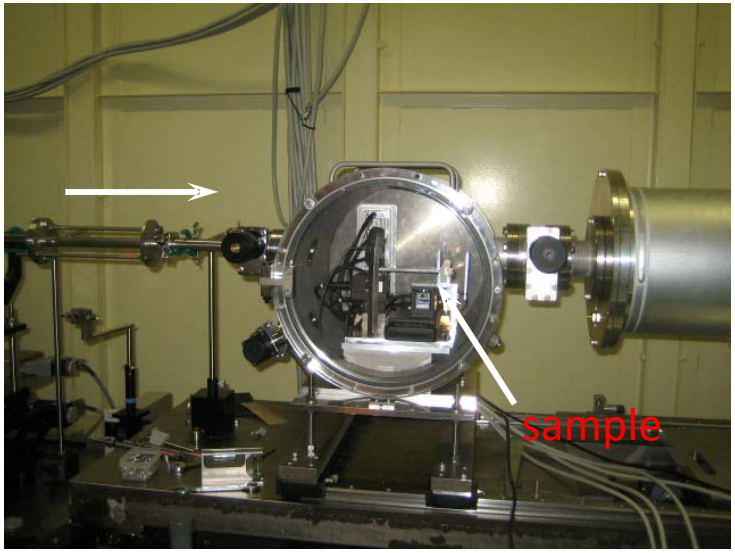

Increase the S/N ratio by 10^2 -10^3.

Masunaga et al, submitted.

-S/N 10-100 times.
-Low BG at high *q*.
-No peaks from the kapton window
-Low noise around beam stopper

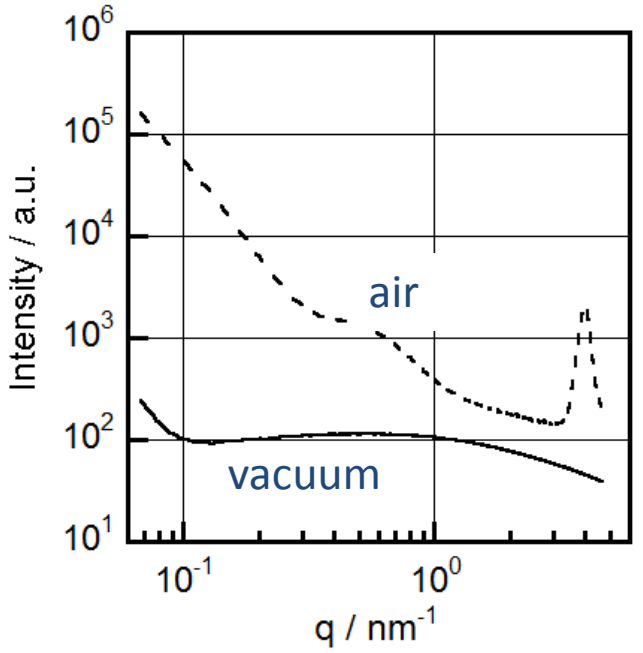

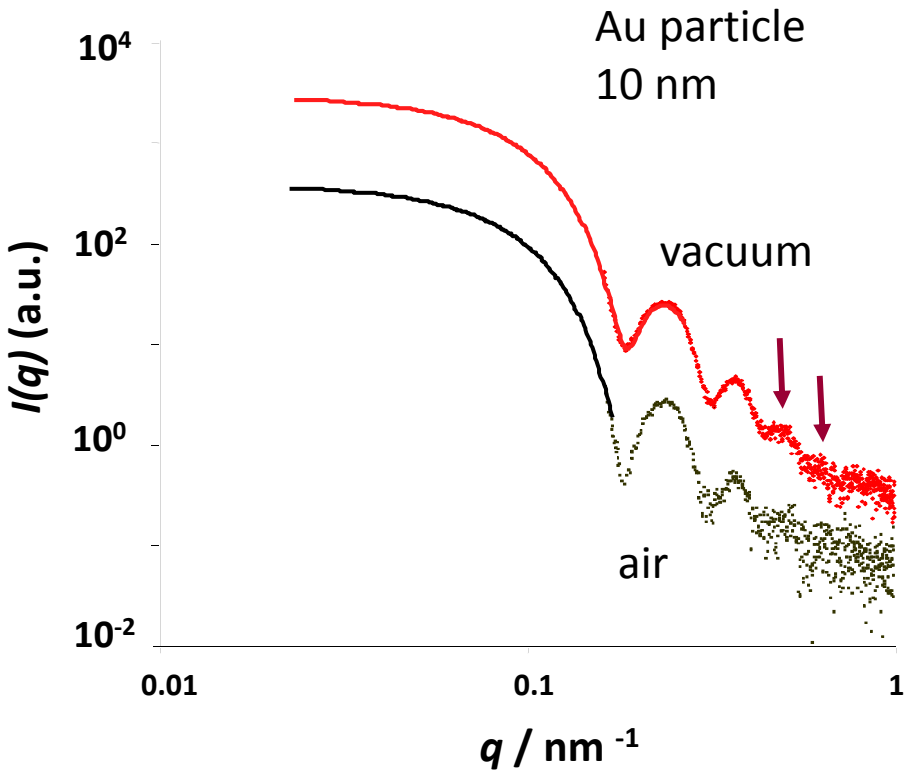

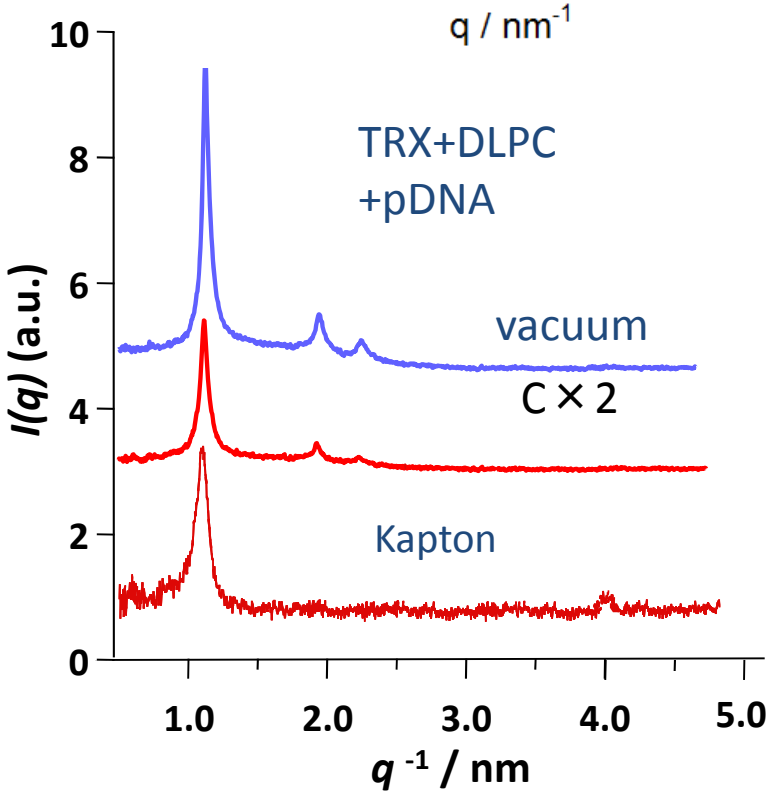

SAXS vs ASAXS

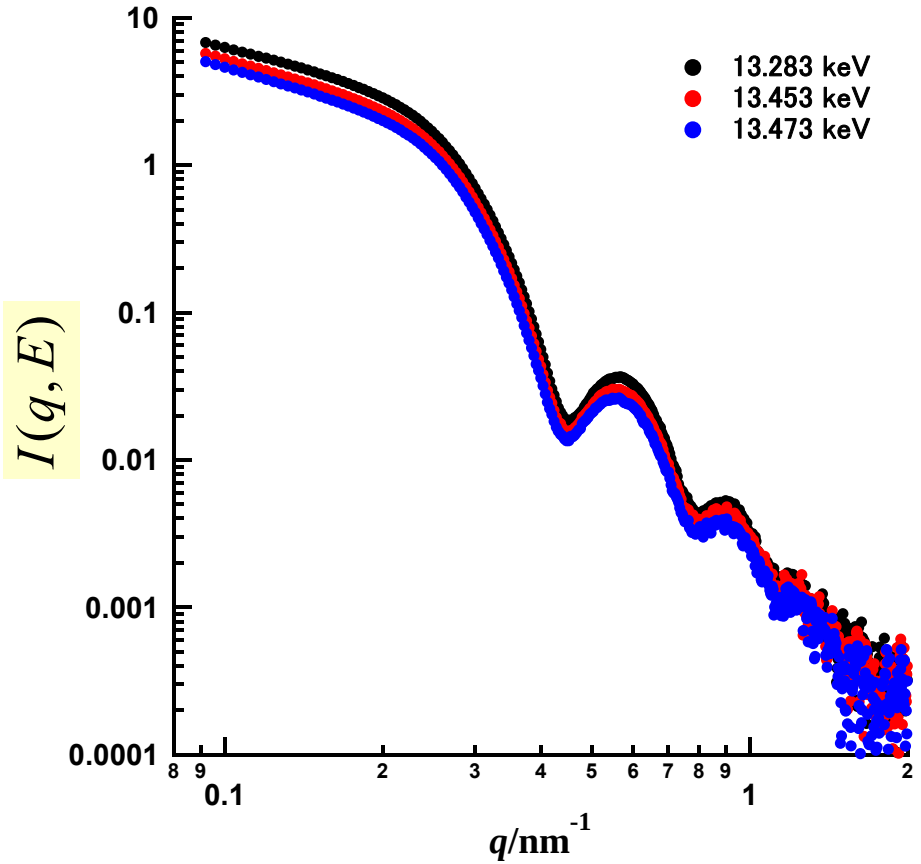

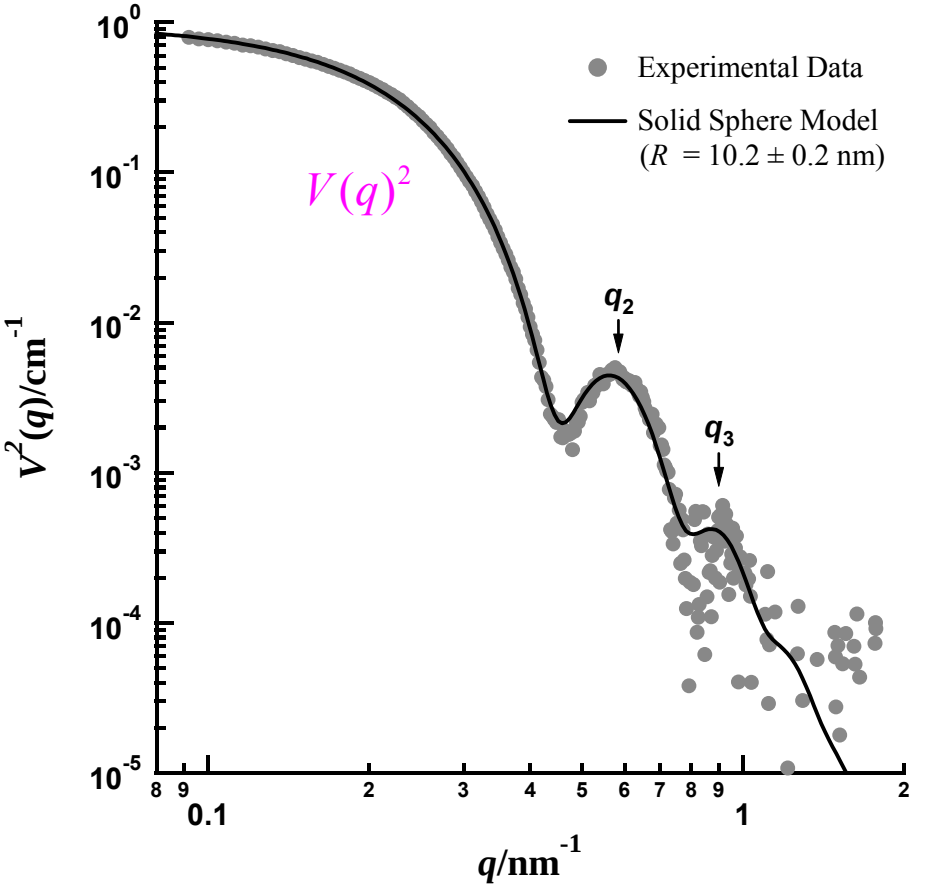

$$I(q) + 2f'(E)U(q)V(q) + [f'^2 + f''^2]V(q)^2$$

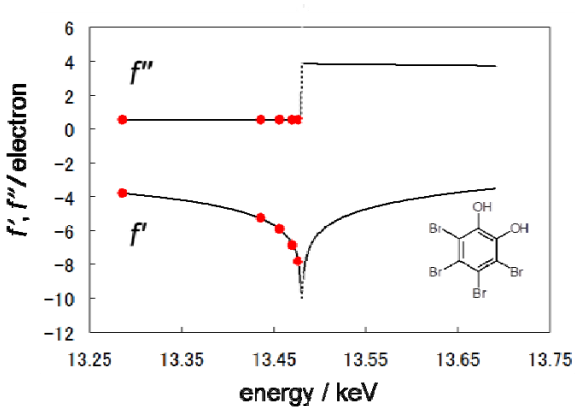

Scattering between Overall Micelle and Br

(1) v^2 term can be fitted with a simple hard-sphere model

(2) The core is smaller than the Br- hard sphere

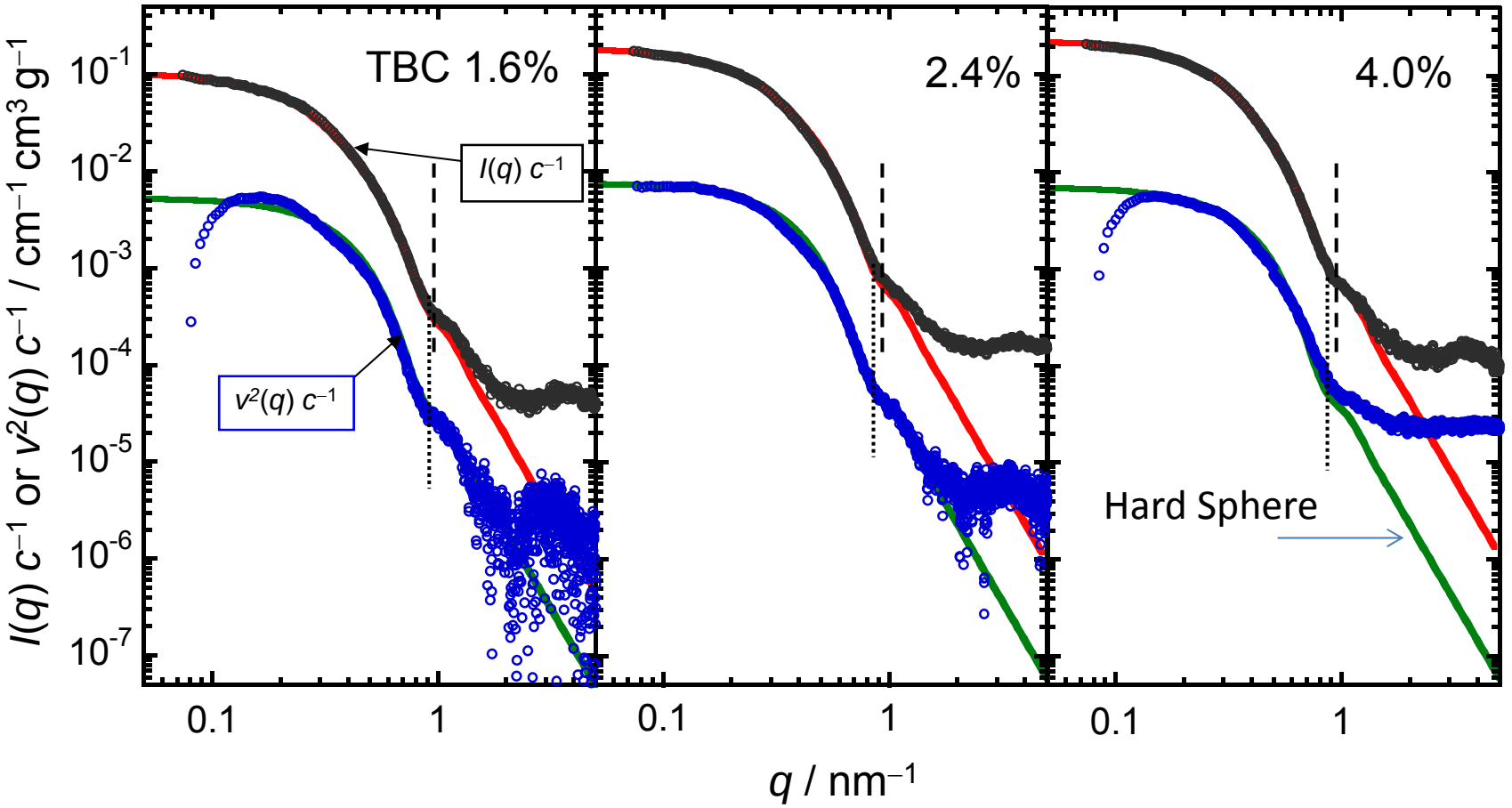

SAXS profiles (black circles), resonant terms of the polymeric micelles (blue circles), and theoretical curves calculated from hard sphere models

Other modeles

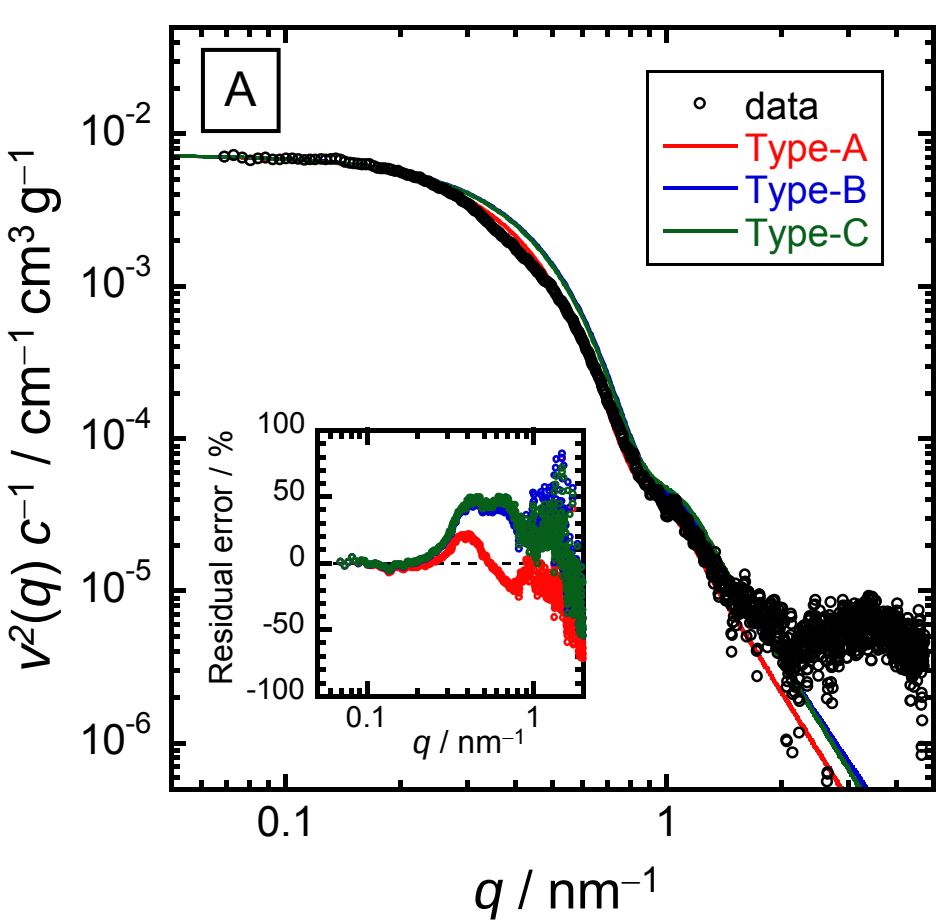

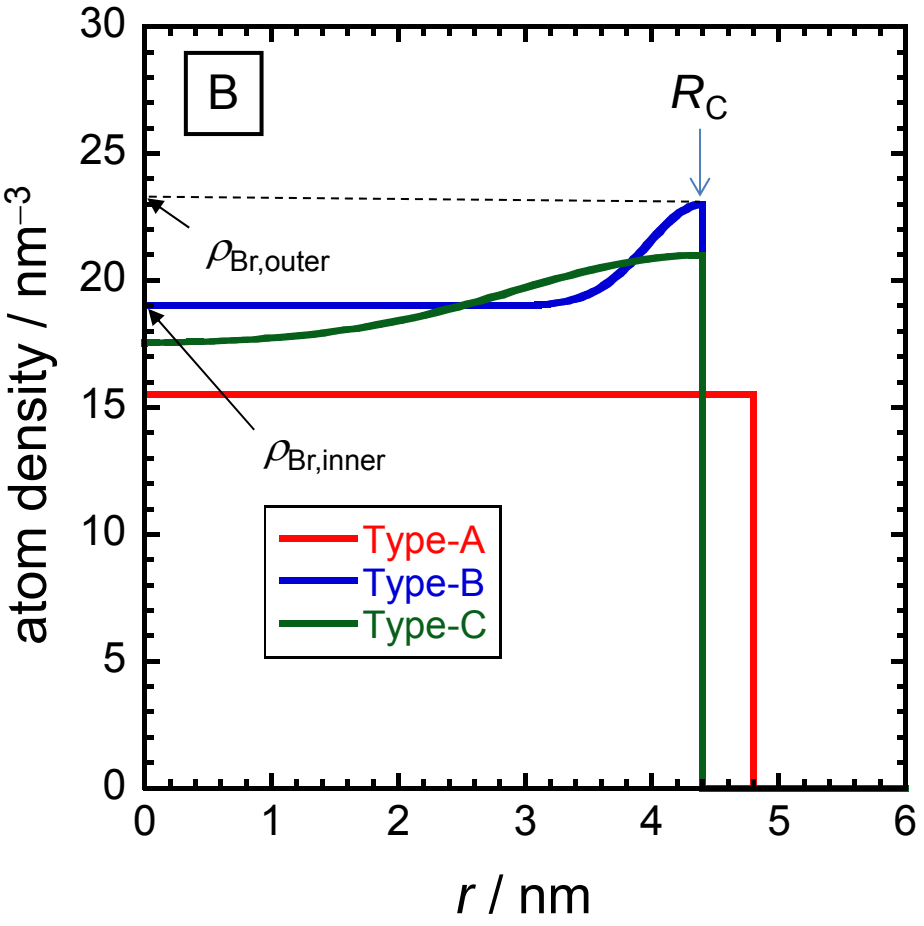

TCB is Infiltrating into the PEG Domain

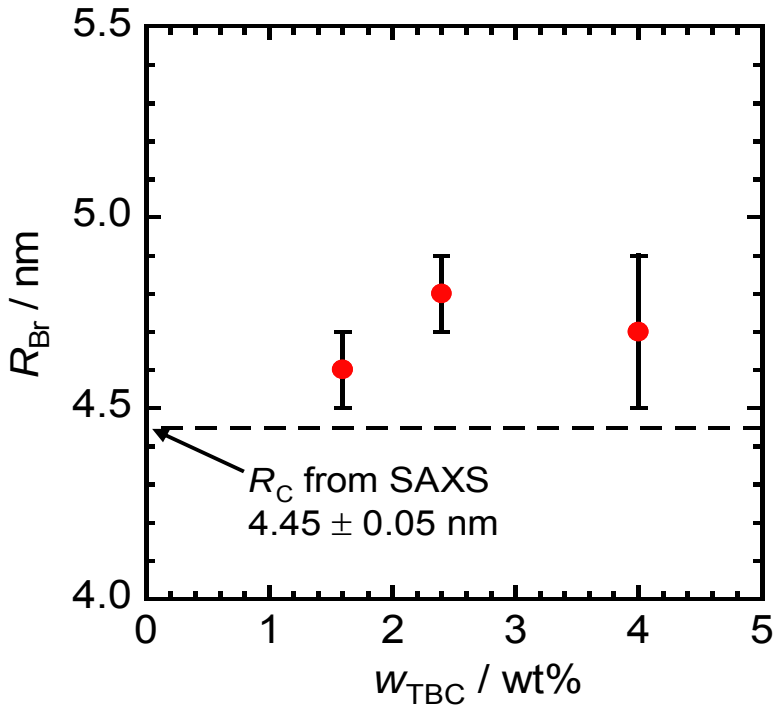

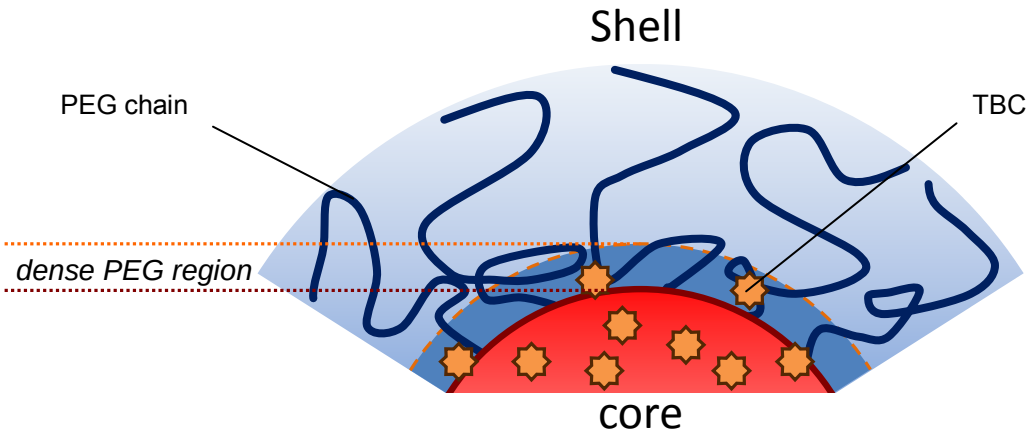

TBC distribution in the micelle. TBC is smearing into the PEG densely-packed interface. Probably, because PEG is partially dehydrated due to the overcrowding.

Summary

Overall:

- The core-chain's hydrophobicity is the major factor to determine the aggregation number and thus core size.
- N_{agg} = 30- 40 at BI = 80%➔ 100 at 90%
- At the same hydrophobicity, the scaling theory describes the chain length dependence of *R*c and *R*s.

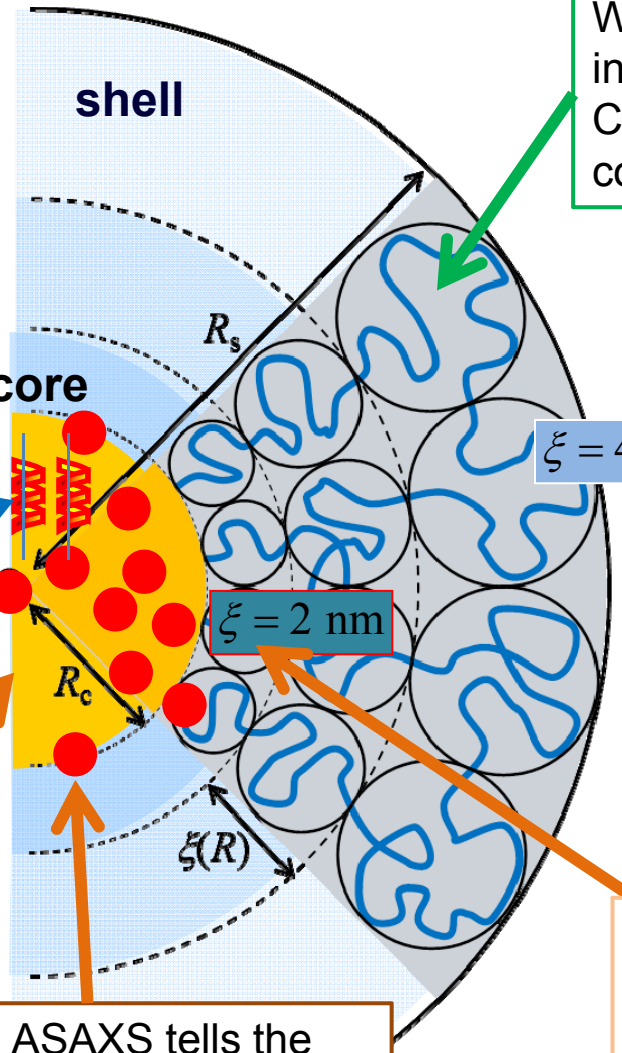

Water/shell interface
Close to the isolate conformation.

$2Rg = 6$ nm

$\xi = 4-5$ nm

$\xi = 2$ nm

ζ : Blob length

Long period exists.
Drug-loading erases the ordering.

The drugs are uniformly distributed in the core.

ASAXS tells the drug smears out to the PEG phase.

core/shell interface
Condensed , 3-5 times, but not to fully stretched.

Outline

Self-assembly and Drug Delivery System (DDS)

Strength of SAS technique in exploring DDS particles

Examples from Our Recent Studies

- Polymeric Micelle for Delivering Hydrophobic Drugs

J. Am. Chem. Soc., 135 (7), 2574–2582(2013)
Macromolecules, (Web): July 23, (2012)
J. Phys. Chem. B, 8241–8250, (2012)
Polymer Journal, 44, 240-244 (2012)

- Monodisperse Calixarene Micelles for DNA Delivery

Langmuir, *28* (6), 3092–3101, (2012)
Bull. Chem. Soc. Jpn. 354-359 (2012)
Langmuir, 29 (45), 13666–13675,（2013）
Chem. Commun.,49, 3052-3054,（2013）

- Short DNA DDS for Immune-stimulation and Gene Silencing

J. Phys. Chem. B,, 116 (1), 87–94 (2012)
Molecular Therapy (Nature), 20, 1234-1241 (2012)
Journal of Controlled Release, 155-161 (2011)
Bioconjugate Chemistry 22 9-15, (2011)
J. Am. Chem. Soc. 126, 8372-8373, (2004)

Outline

Self-assembly and Drug Delivery System (DDS)
Strength of SAS technique in exploring DDS particles

Examples from Our Recent Studies

- Polymeric Micelle for Delivering Hydrophobic Drugs

J. Am. Chem. Soc., revision submitted
Macromolecules, (Web): July 23, (2012)
J. Phys. Chem. B, 8241–8250, (2012)
Polymer Journal, 44, 240-244 (2012)

- Monodisperse Calixarene Micelles for DNA Delivery

Langmuir, *28* (6), 3092–3101, (2012)
Bull. Chem. Soc. Jpn. 354-359 (2012)

- Short DNA DDS for Immune-stimulation and Gene Silencing

J. Phys. Chem. B,, 116 (1), 87–94 (2012)
Molecular Therapy (Nature), 20, 1234-1241 (2012)
Journal of Controlled Release, 155-161 (2011)
Bioconjugate Chemistry 22 9-15, (2011)
J. Am. Chem. Soc. 126, 8372-8373, (2004).

Topoic 2: Shape Persistence Micelles for DNA Delivery

DNA transfection
Cationic lipids

DOTAP

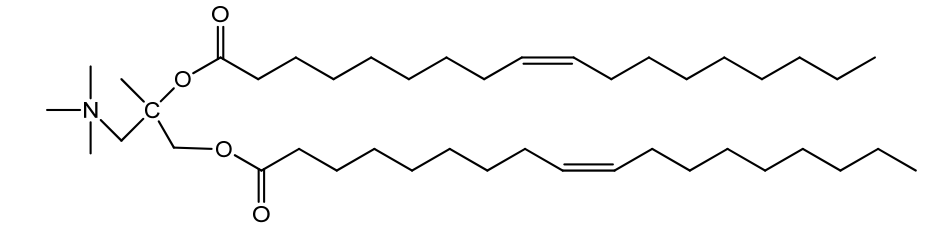

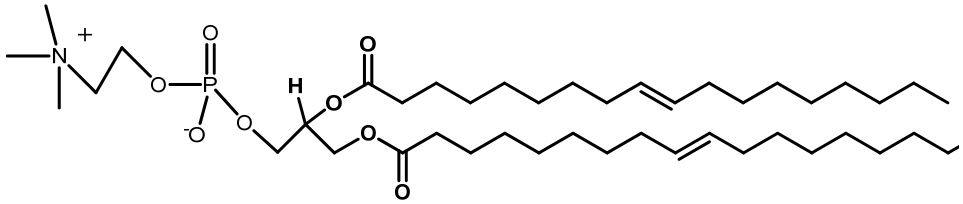

DOPE

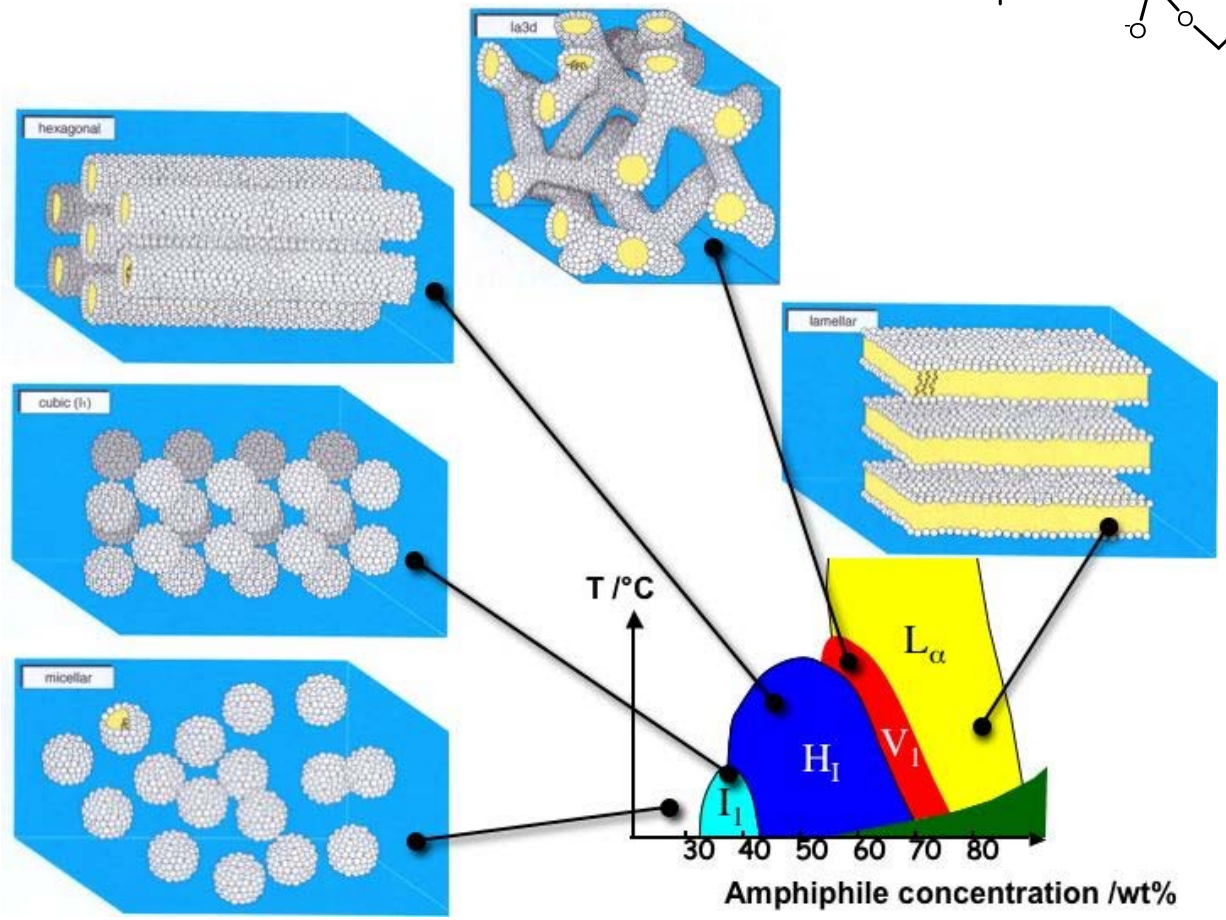

Structure is important to control transfection efficiency.

But, its control is difficult.

Cholic Acid Micelle (or Aggregate): no rule without an exception

cholic acid

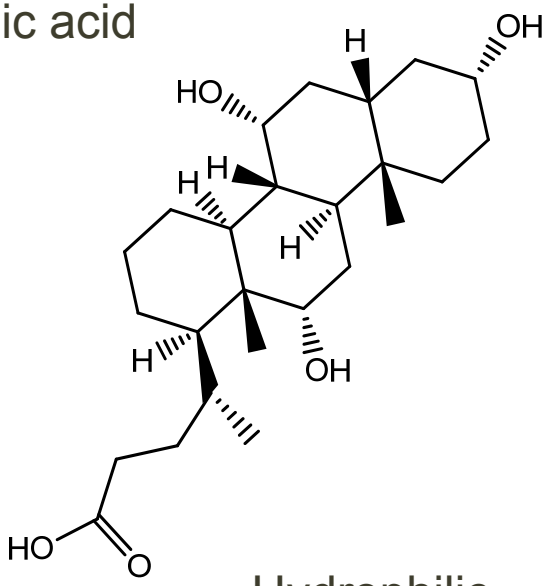

Hydrophilic

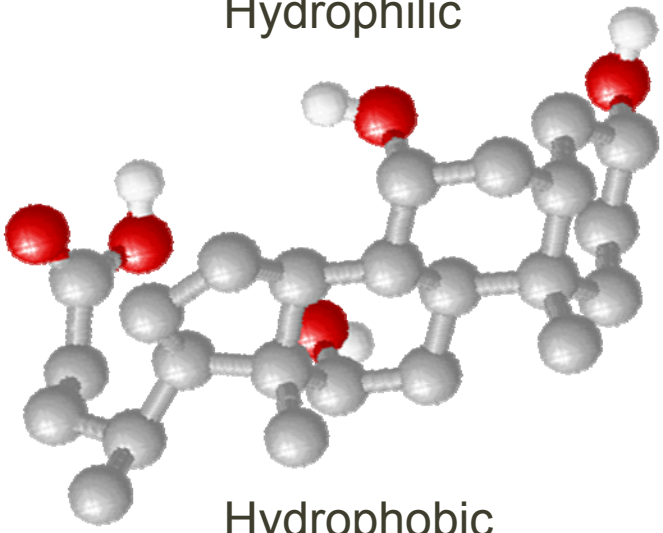

Hydrophobic

In aqueous solution,
Dimerization

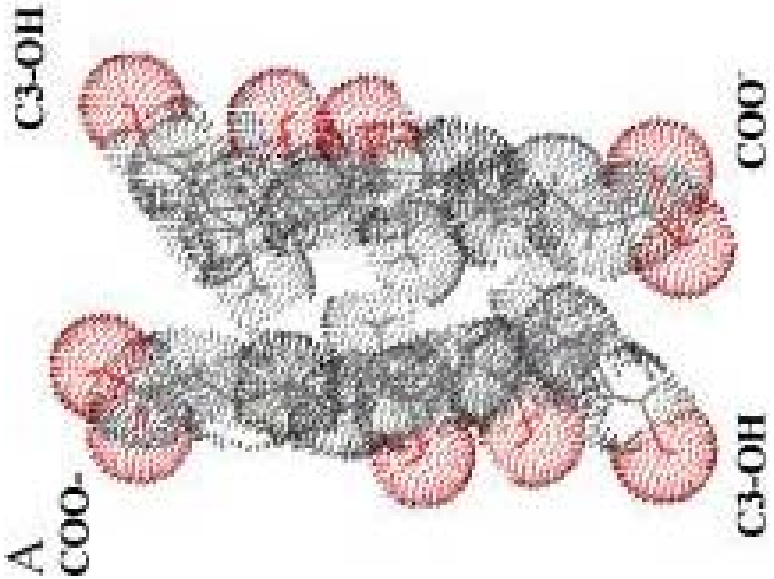

Colloids and Surfaces B: Biointerfaces 285–291

Cholic acid, along with chenodeoxycholic acid, is one of two major bile acids produced by the liver.

Flexible to Rigid

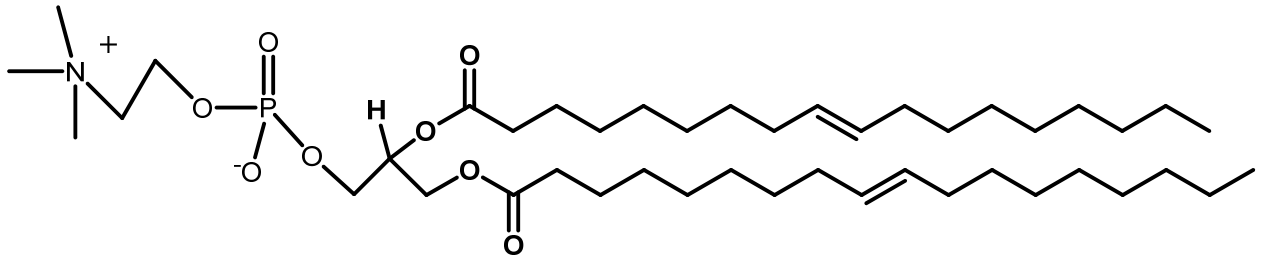

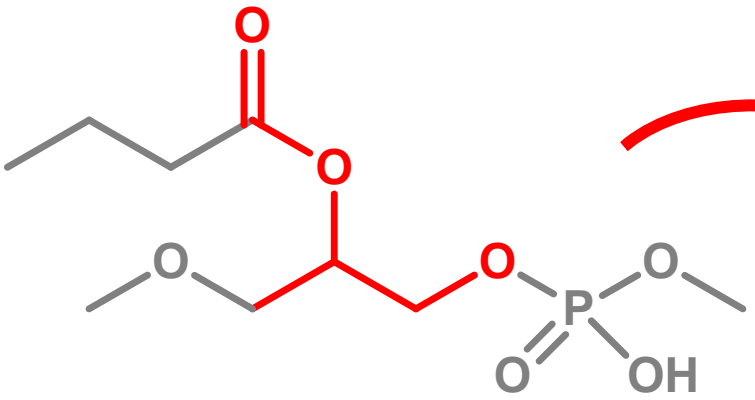

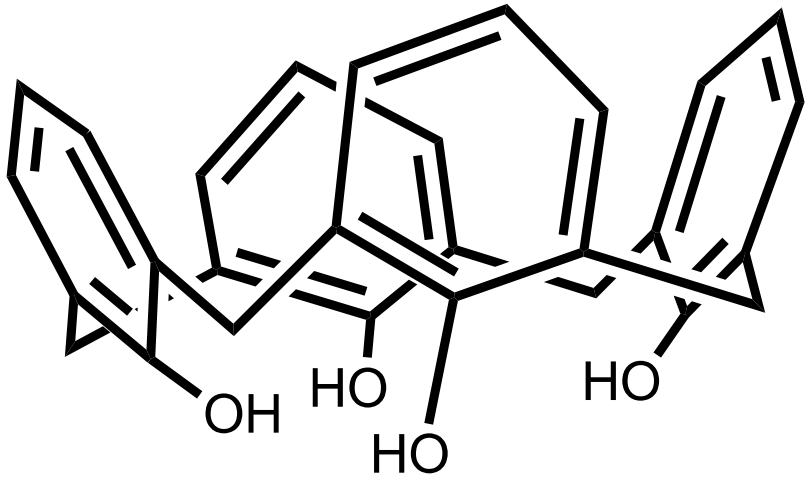

Flexible junction point

Rigid Calix[4]arene

➔ cationic lipids for DNA delivery

Synchrotron Small Angle X-ray Scattering

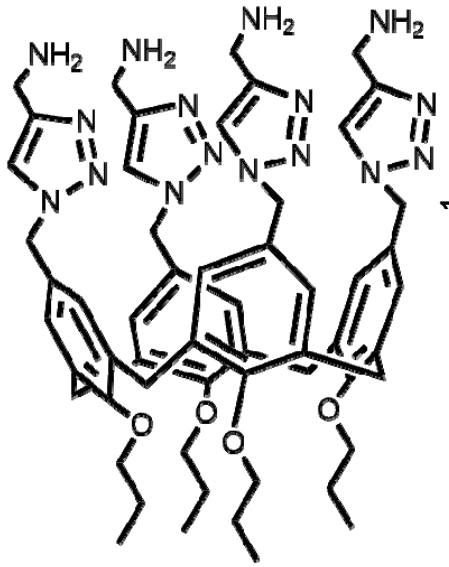

CaL[4]C3

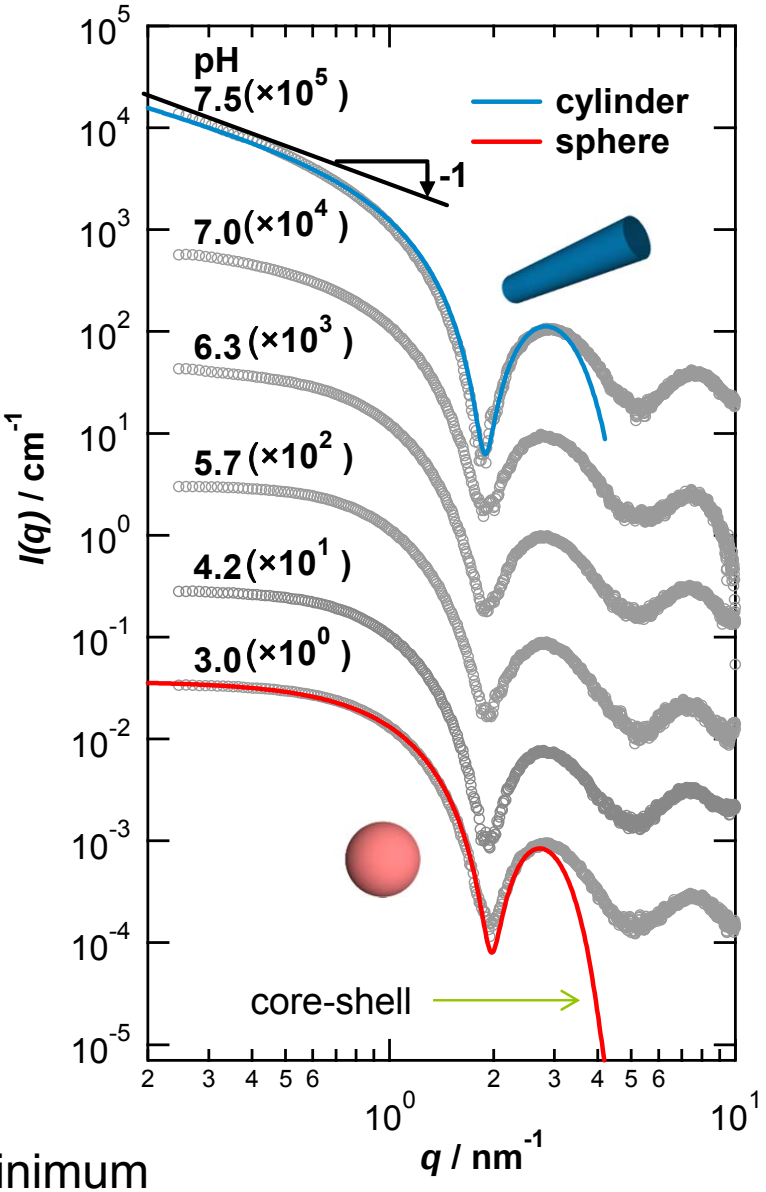

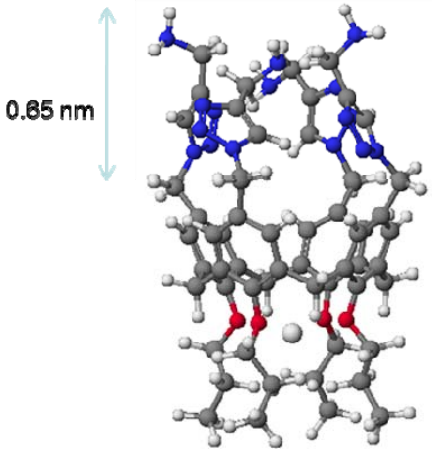

deprotonated

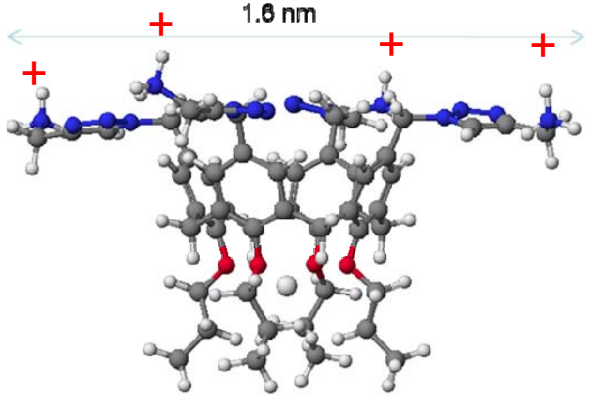

protonated

At low pH, sharp minimum

➔ Mono-dispersity and high symmetry

AFM

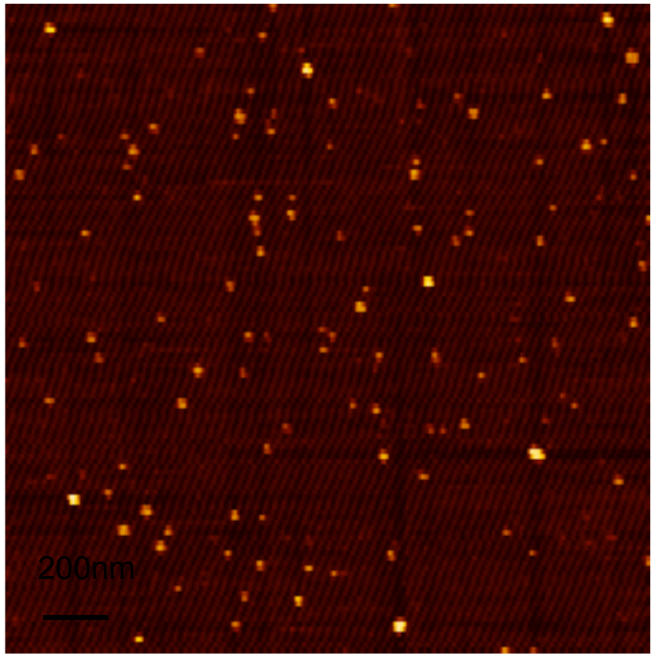

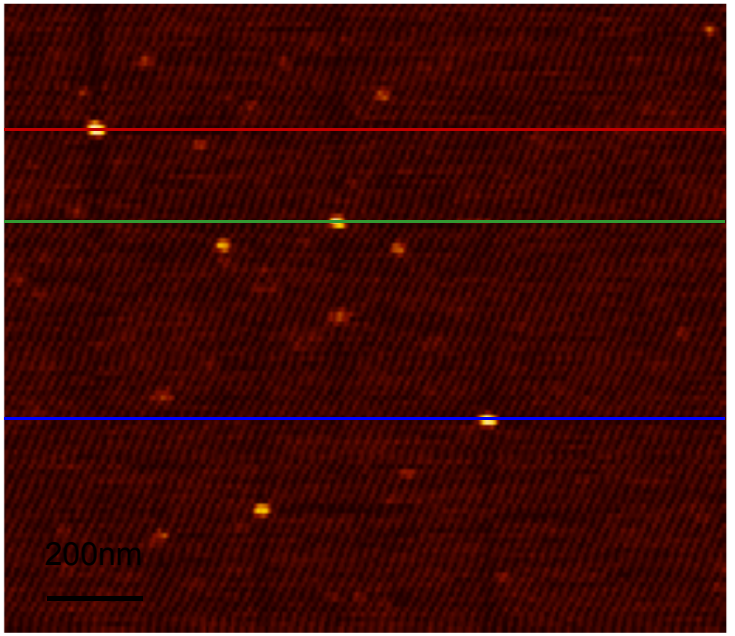

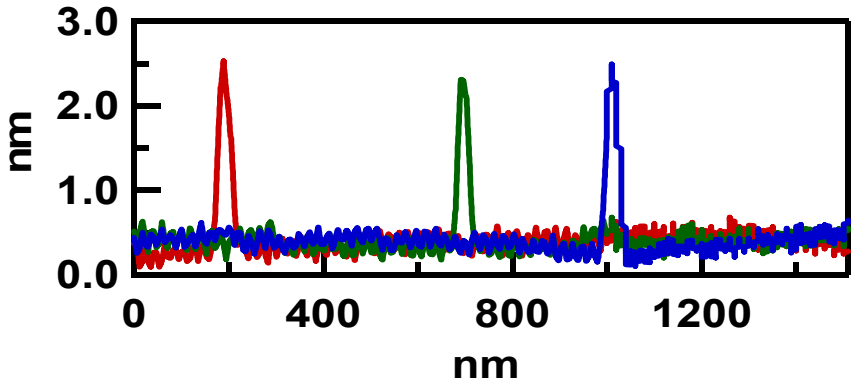

Na Specificity of the sharp minimum of the intensity

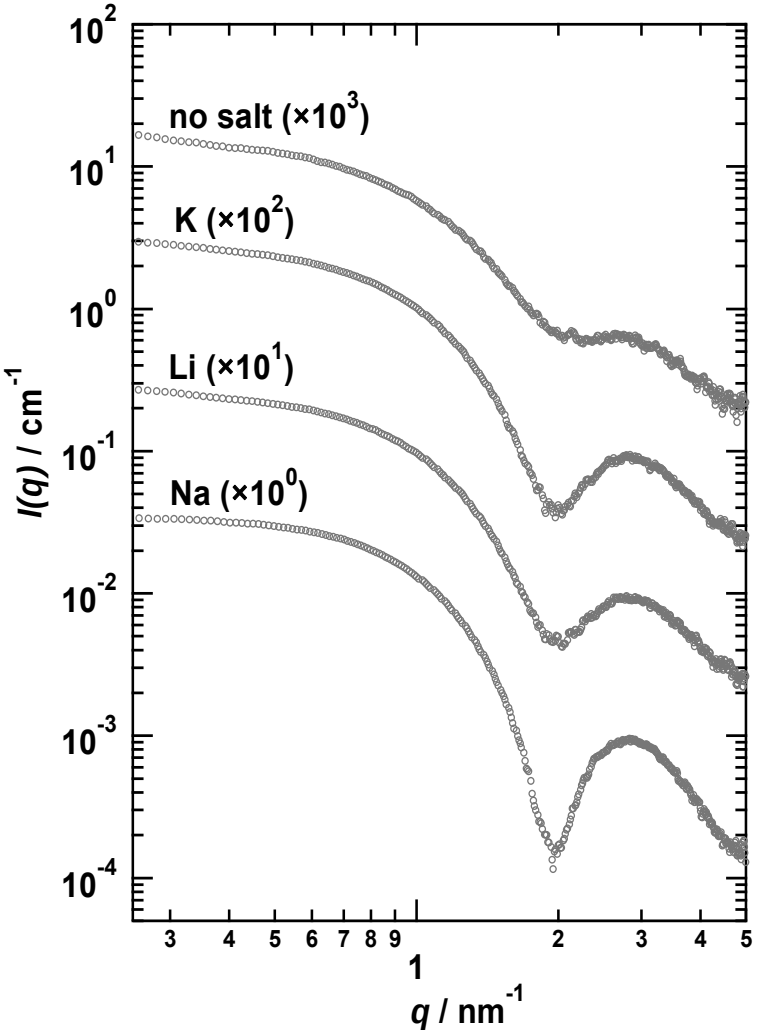

Cation dependence

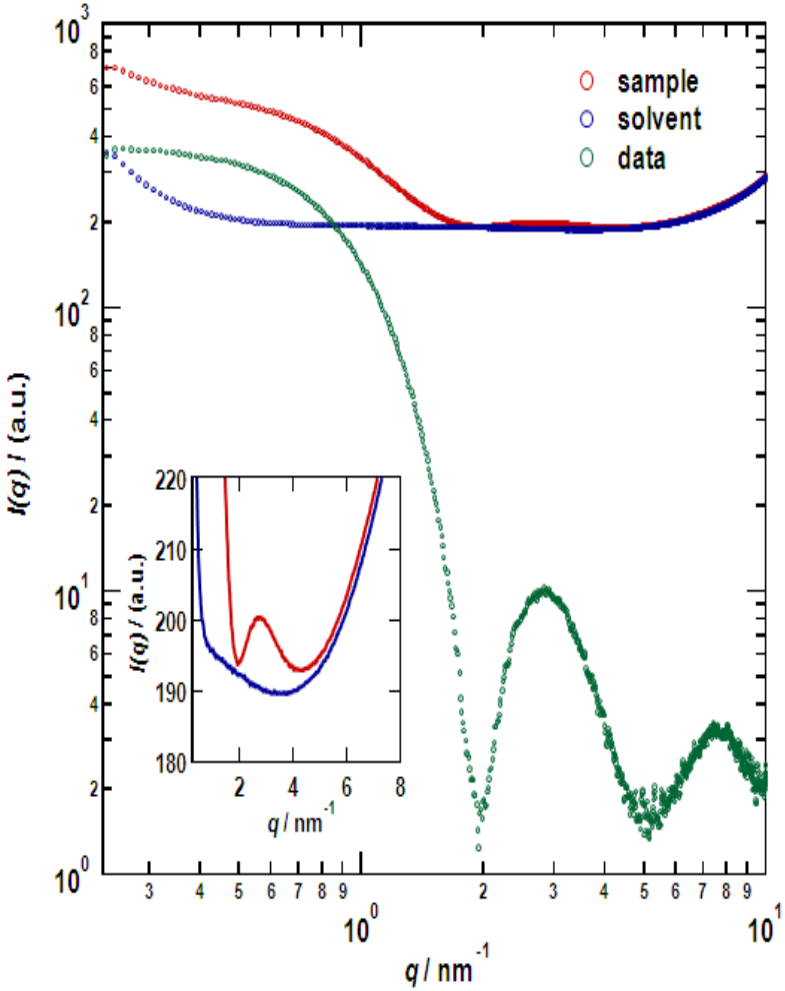

The sharp minimum is not due to artificial effect in the solvent subtraction.

FFF-MALS

Sample concentration : 10 mg/mL, solvent : 50 mM NaCl (pH = 3.0),
Flow conditions : constant flow (4mL/min), Wavelength : 270 nm

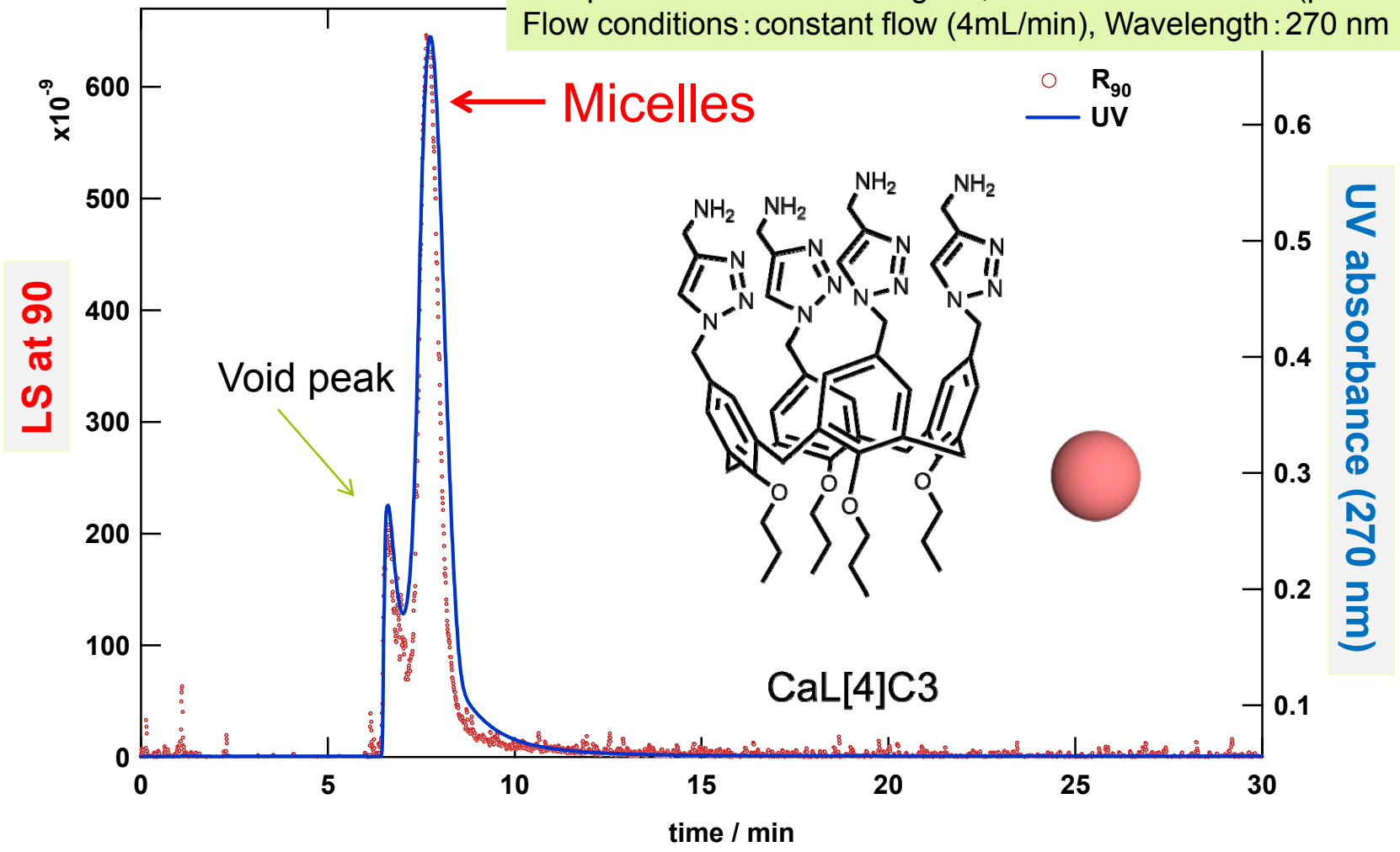

- Micelle peak is only one → No aggregation
- The red and blue data are almost completely overlapping with each other.
- Molar mass = 5.7×10^3 ➔ Aggregation number is 6

FFF for Cal[4]C6

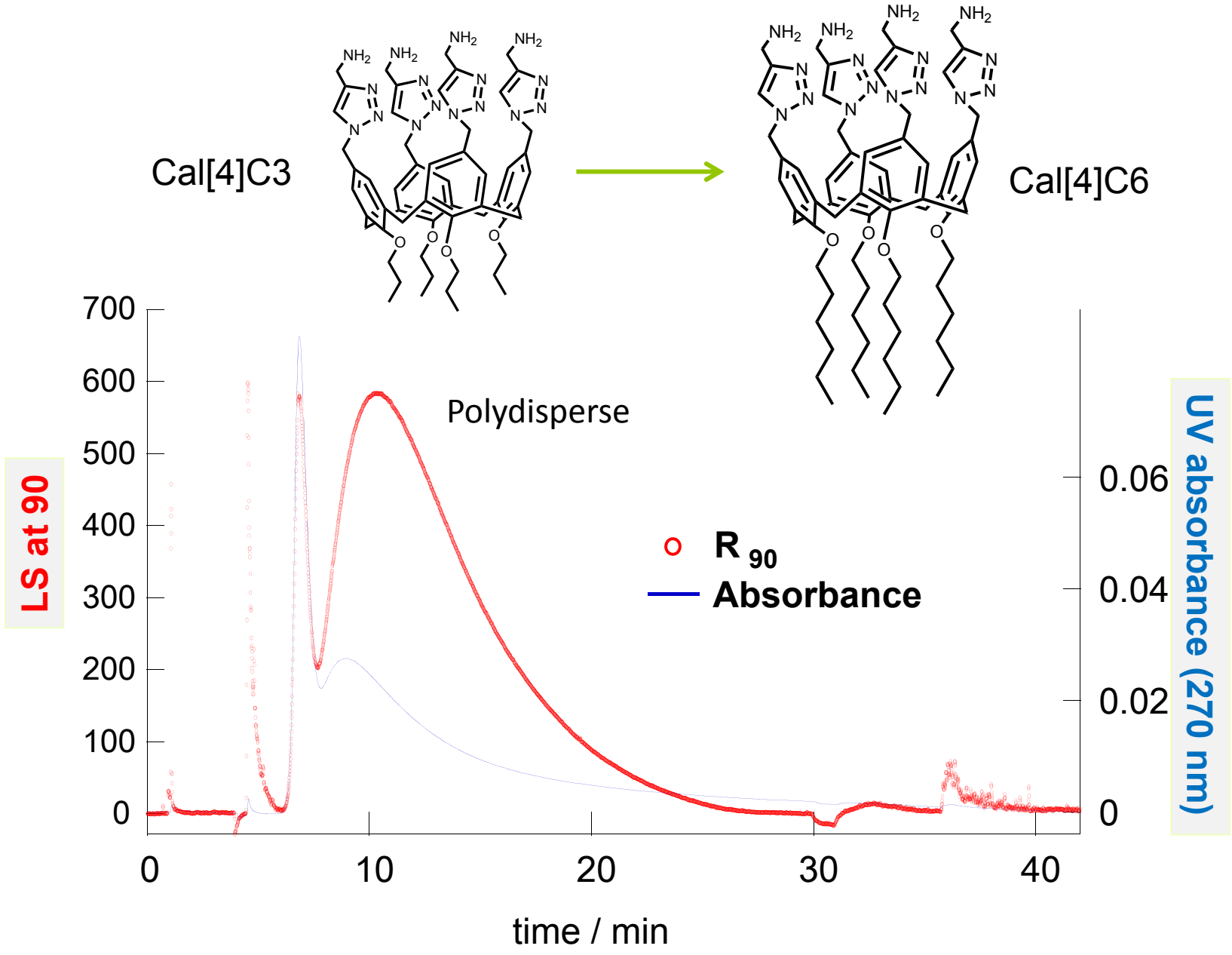

Molar Mass Determination

$$I(0) = NV_M{}^2(\bar{\rho} - \rho_0)^2 = \frac{M_M}{N_A} C_M \bar{v}^2 (\bar{\rho} - \rho_0)^2$$

$\bar{\rho} - \rho_0$ can be calculated from the atomic scattering factor .

$\bar{v}$ by measuring the density increment

Need an assumption !
No information about the distribution

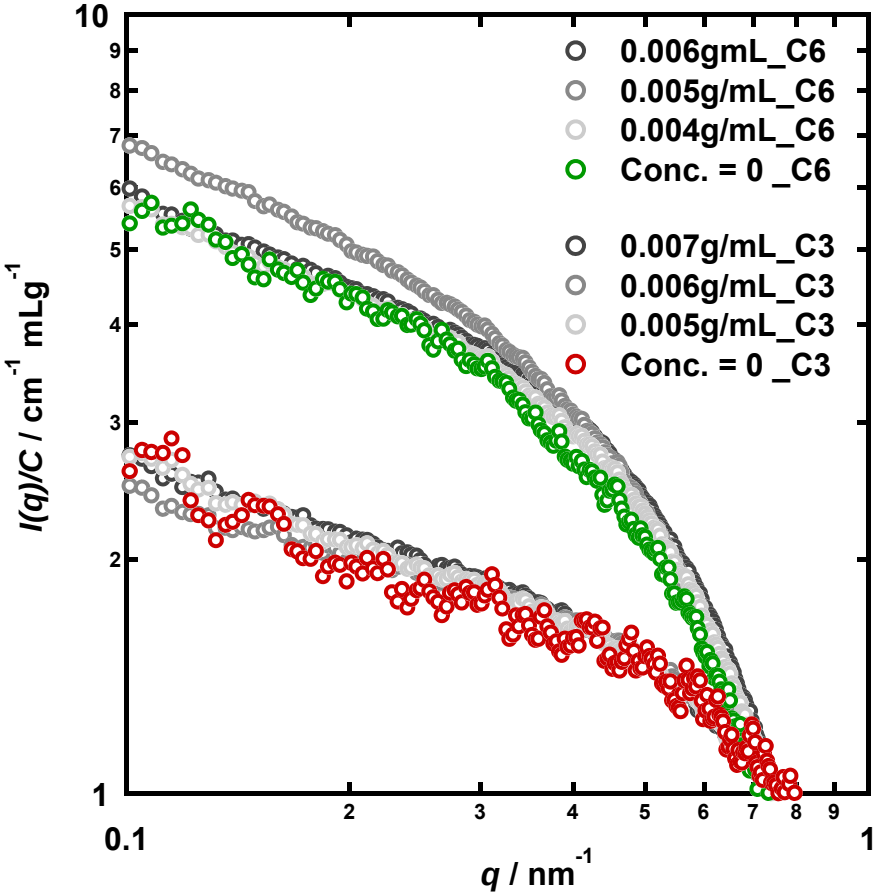

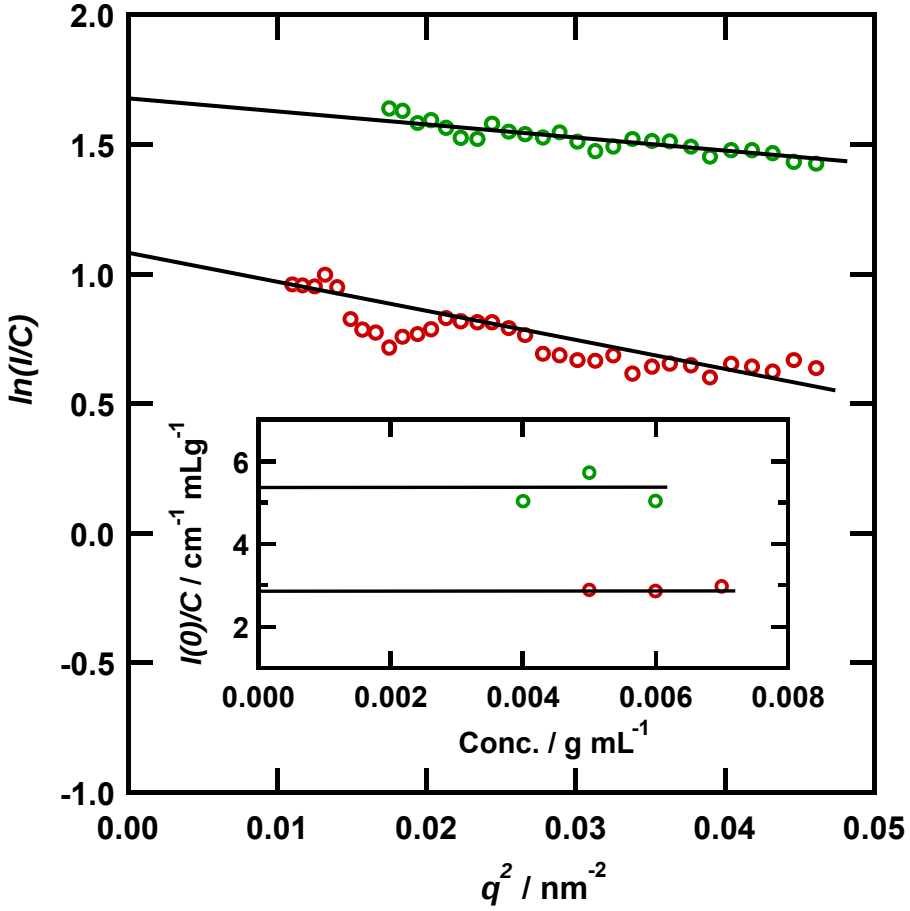

The molar masses of C3 and C6 are **600 and 14800**.

Molar Mass and Distribution with Three Different Methods

The molar masses determined with different methods and the aggregation numbers.

sample	SAXS	FFF+MALS		AUC		Aggregation number
	M_w / 10^3	M_w / 10^3	M_w/M_n	M_w / 10^3	M_z/M_w	
CaL[4]C3	6.00 ± 0.20	5.69 ± 0.93	1.00_7	6.10 ±0.20	1.0_7	6
CaL[4]C6	14.8 ± 0.95	13.0 – 20	1.5	14.7 ± 0.90	1.5	10 - 16

SAXS: synchrotron small-angle X-ray scattering.
LS: static light scattering.
AUC: analytical ultracentrifugation

Sphere or Cubic ?

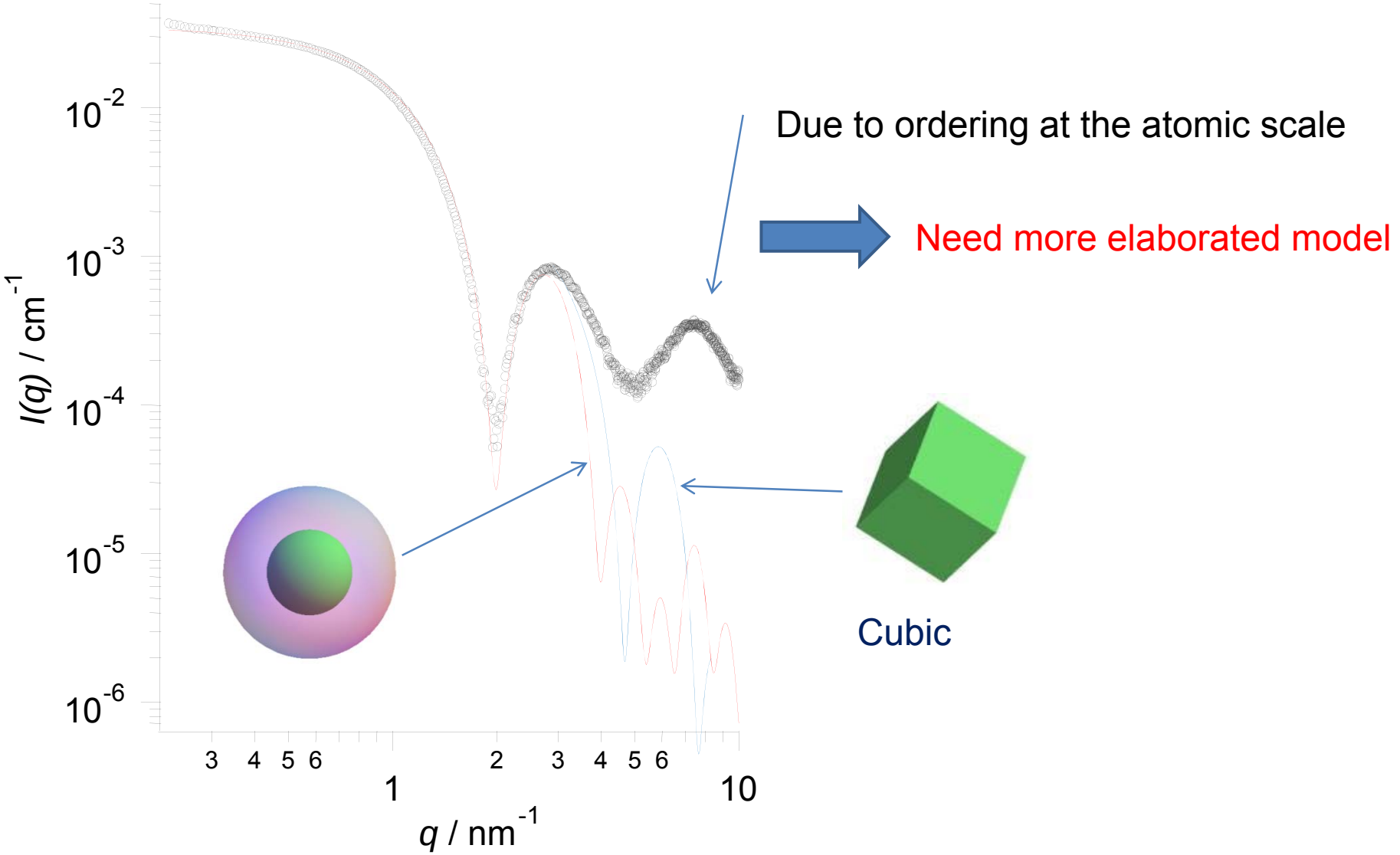

Shape Determination with Dummy Atom Model

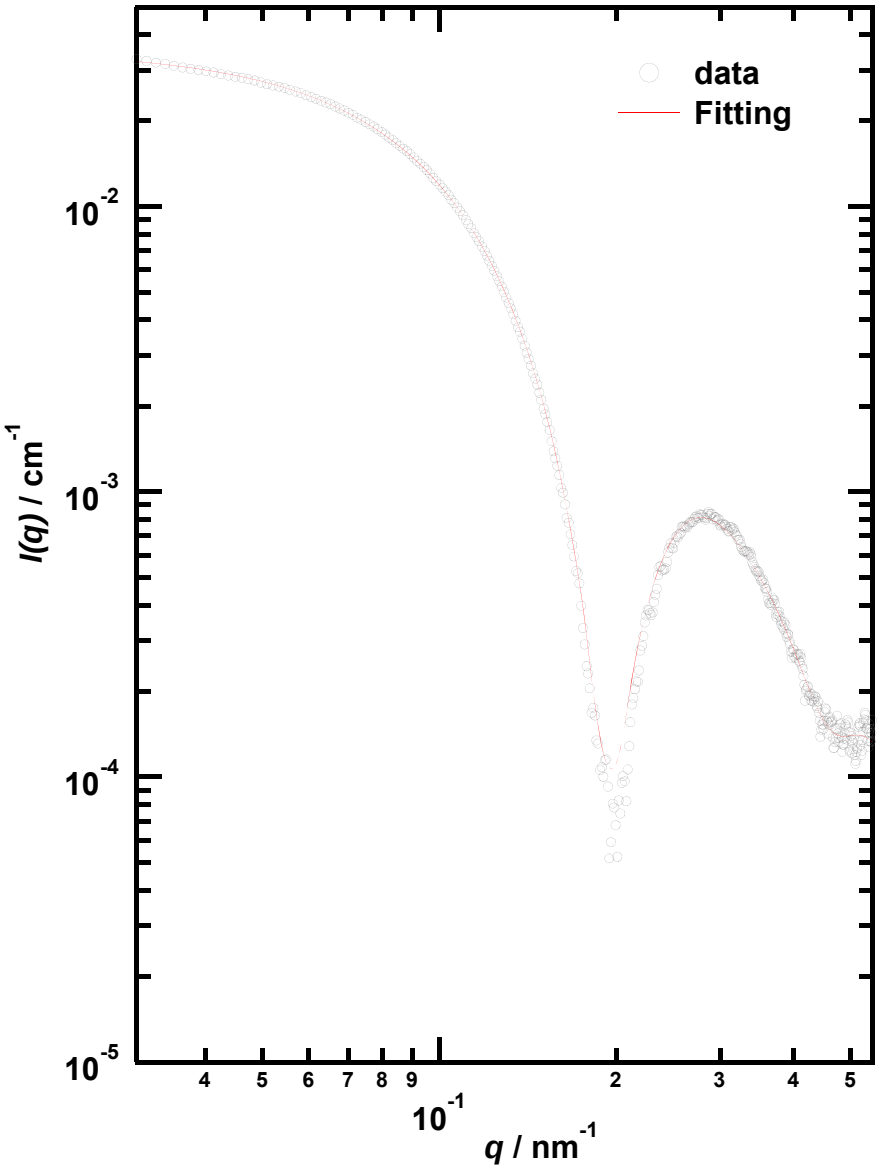

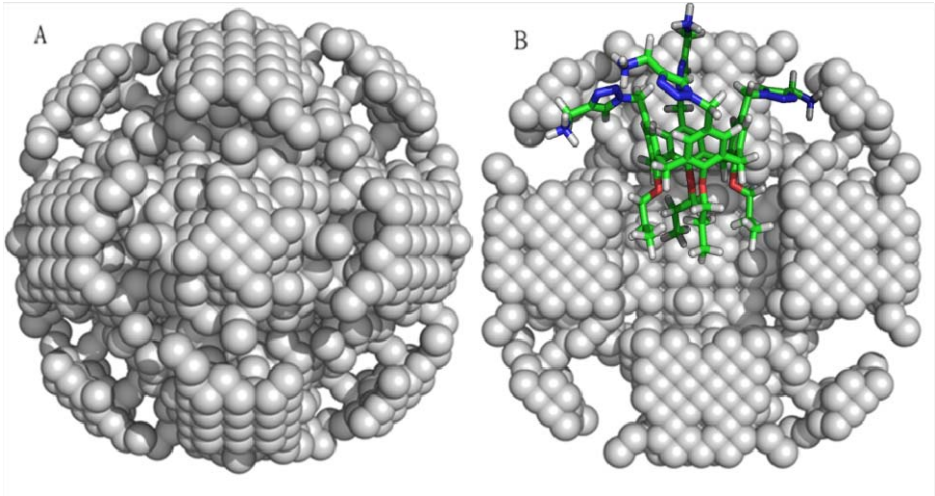

(Cross section)

Ab initio Shape Determination by Simulated Annealing using Bead Model Restriction: cubic symmetry (Dmitri Svergun)

At low pH and presence of Na^+ or K^+

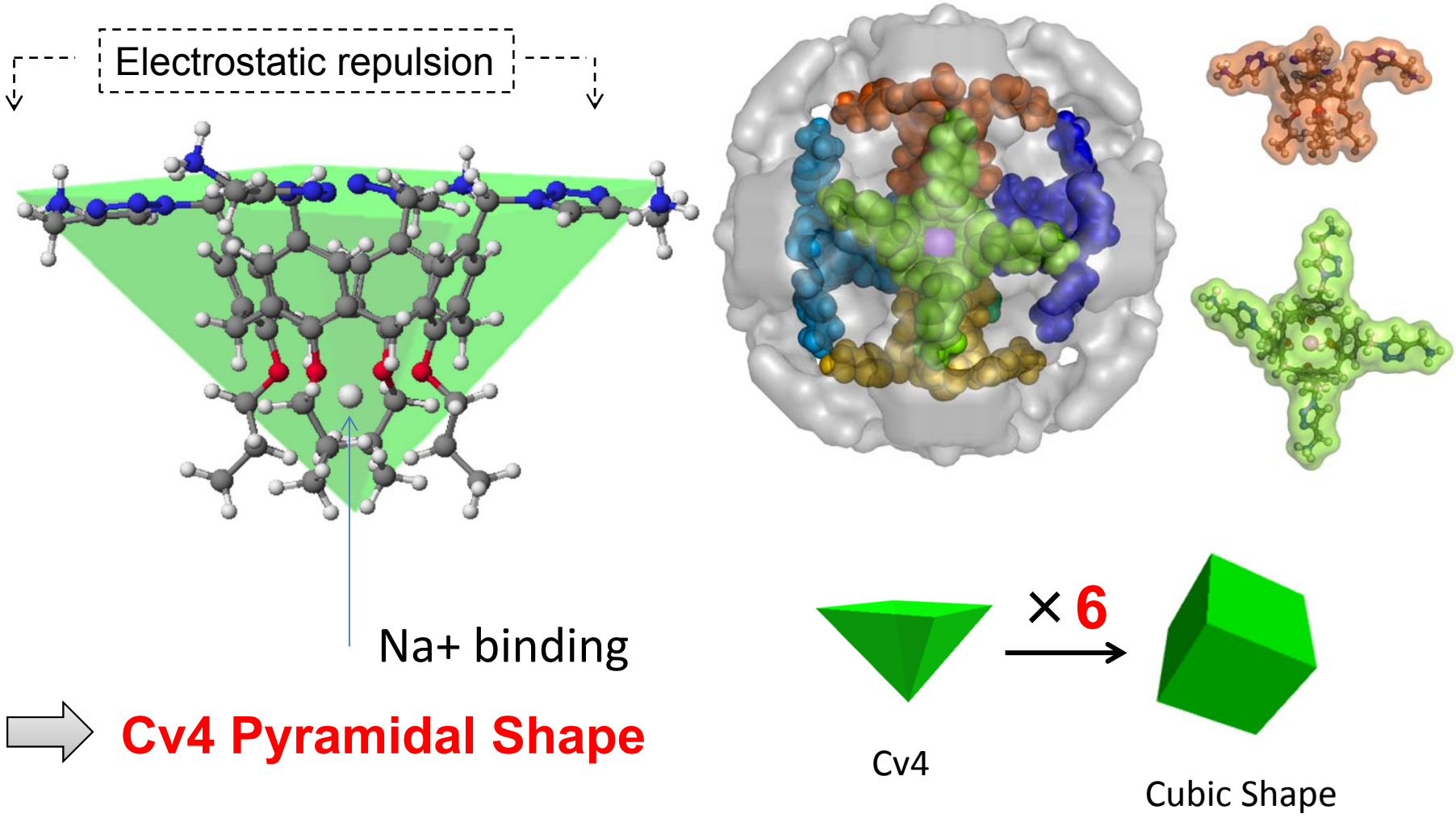

Fujii et al., *Langmuir,* 2012, 28 (6), 3092–3101